Mixing of Ionic and Covalent Configurations for NaH, KH, and MgH^+. Potential Energy Curves and Couplings between Molecular States[1a]

Robert W. Numrich and Donald G. Truhlar*[1b]

Department of Chemistry, University of Minnesota, Minneapolis, Minnesota 55455 *(Received June 12, 1975)*

Configuration mixing between ionic and covalent configurations in the hydrides NaH, KH, and MgH^+ has been studied using a two-electron valence bond model in which the valence electrons are assumed to interact with the metal core through a Hellmann-type pseudopotential. Adiabatic potential energy curves are reported for the $X^1\Sigma^+$, $A^1\Sigma^+$, $B^1\Sigma^+$, $a^3\Sigma^+$, $b^3\Sigma^+$, $c^3\Sigma^+$, $^1\Pi$, and $^3\Pi$ states arising from the ns, np, and $(n+1)$s atomic states of the metal atoms. For each hydride a polarization potential was added to the diabatic ionic potential curve and this potential was adjusted in such a way that the binding energy of the $A^1\Sigma^+$ adiabatic state is in good agreement with the experimental value. The $A^1\Sigma^+$ potential energy curves are also in good agreement with RKR curves determined from experiment although they are shifted slightly to larger values of the internuclear distance. For each diatomic system, coupling matrix elements between electronic states were calculated in a nonorthogonal diabatic representation, in a symmetrically orthogonalized diabatic representation, and in the adiabatic representation. The elements of the nonorthogonal diabatic Hamiltonian matrix and the overlap matrix were used to calculate the Landau–Zener–Stueckelberg parameter ΔW which is the separation between adiabatic potential energy curves at the position of an avoided crossing in a two-state approximation. Comparison with values of ΔW obtained earlier by Bates and Boyd and by Grice and Herschbach shows fair agreement between the values obtained here and those obtained by Bates and Boyd while the values obtained by Grice and Herschbach are two to three times larger. The elements of the nonorthogonal diabatic Hamiltonian matrix and the elements of the inverse square root of the overlap matrix were fit to analytic forms as functions of the internuclear distance. These forms were used to evaluate the part of the coupling matrices between adiabatic states which arises from the R dependence of the transformation matrices between the three electronic representations. The results show that coupling between adiabatic states in these molecules is important over intervals as large as 10 bohrs and serious questions are raised concerning the Landau–Zener–Stueckelberg model for treating the problem of avoided crossings in scattering calculations involving these systems.

I. Introduction

Interest in the electronically inelastic scattering of alkali atoms and alkali-like ions has been strong in recent years due to improved experimental techniques for measuring such processes and the fact that electronically excited states of these atoms and ions are amenable to quantum theoretical treatment.

In the work reported in this paper the valence bond configuration mixing method was combined with the use of model atomic pseudopotentials in calculations of the potential energy curves and the matrix elements which couple different electronic states of NaH, KH, and MgH^+ in both adiabatic and diabatic representations. Since the coupling terms have not been well studied, this work seeks to determine their general features as functions of internuclear distance.

This work was carried out as the initial stage of scattering calculations for electronically inelastic collisions of Na, K, and Mg^+ with H and H_2. The calculations are also of intrinsic value, especially for illustrating the nature of the coupling terms and the diabatic potential energy curves and for showing the level of accuracy which can be achieved for adiabatic potential energy curves using this method.

The Landau–Zener–Stueckelberg (LZS) model[2] for electronically inelastic collisions has been applied to two of the avoided crossings in each of the systems NaH and KH by Bates and Boyd[3] and the treatment has been repeated in modified fashion for one of the avoided crossings in each system by Grice and Herschbach.[4] This model requires the energy separation ΔW between adiabatic potential energy curves at an avoided crossing. Although the primary purpose of this work is not to apply the LZS model, we are able to calculate ΔW within our treatment and we shall compare our results for this quantity with the results reported in the references cited.

II. Electronic Representations

For a fixed value of the internuclear distance R we consider the electronic Hamiltonian

$$H_{el}(R) = \frac{1}{2\mu_e}\sum_{i=1}^{n} p_{x_i}^2 + V(\vec{x}, R) \tag{1}$$

where

$$\frac{1}{\mu_e} = \frac{1}{(M_A + M_B)} + \frac{1}{m} \tag{1a}$$

m is the electronic mass, $\hat{p}_{x_i}$ is the operator for linear momentum of electron i, $\hat{x}_i$ is the coordinate of electron i in a molecule-fixed coordinate system with origin at the center-of-mass of the nuclei, $\hat{x}$ represents the entire set of electronic coordinates, and V is the total potential energy consisting of electron–nucleus attractions, electron–electron repulsions, and nucleus–nucleus repulsions. We also consider the eigenvalue problem

$$H_{el}(R)\phi_k(\vec{x}, R) = W_k(R)\phi_k(\vec{x}, R) \tag{2}$$

with eigenvalues $W_k(R)$ and electronic eigenfunctions $\phi_k(\vec{x}, R)$ which are taken to be orthonormal as follows

$$(\phi_i|\phi_j) = \int \phi_i^*(\vec{x}, R)\phi_j(\vec{x}, R)\, d\vec{x} \quad (3a)$$

$$= \delta_{ij} \quad (3b)$$

The inner product notation introduced in eq 3a refers to integration over electronic coordinates only and δ_{ij} is the kronecker delta. The total wave function is expanded in terms of these electronic eigenfunctions as

$$\Psi(\vec{x}, \vec{R}) = \sum_{l=1}^{\infty} \phi_l(\vec{x}, R)\chi_l(\vec{R}) \quad (4)$$

where the nuclear motion wave functions $\chi_k(\vec{R})$ are to be determined. We substitute expansion (4) into the Schroedinger equation

$$H\Psi = W\Psi \quad (5)$$

where H is the Hamiltonian in the barycentric coordinate system given by

$$H = \frac{1}{2\mu}p^2 + \left(\frac{1}{M_A + M_B}\right)\sum_{i<j}\vec{p}_{x_i}\cdot\vec{p}_{x_j} + H_{el} \quad (6a)$$

where[5]

$$\vec{p} = -i\vec{\nabla}_R \quad (6b)$$

and

$$\frac{1}{\mu} = \frac{1}{M_A} + \frac{1}{M_B} \quad (6c)$$

We set the kinetic energy of the total center of mass equal to zero so W is the total energy. After multiplication on the left by $\phi_k^*(\vec{x}, R)$ and integration over electronic coordinates, we obtain the following coupled differential equations for the nuclear motion wavefunctions:[6]

$$\frac{1}{2\mu}p^2\chi_k(\vec{R}) + [W_k(R) - W]\chi_k(\vec{R}) + \sum_{l=1}^{\infty}[B_{kl}(R) + G_{kl}(\vec{R})]\chi_l(\vec{R}) + 2\sum_{l=1}^{\infty}\vec{F}_{kl}(\vec{R})\cdot\vec{p}\chi_l(\vec{R}) = 0 \quad (7)$$

where

$$B_{kl} = \left(\frac{1}{M_A + M_B}\right)\left(\phi_k\left|\sum_{i<j}\vec{p}_{x_i}\cdot\vec{p}_{x_j}\right|\phi_l\right) \quad (8)$$

$$\vec{F}_{kl} = \frac{1}{2\mu}(\phi_k|\vec{p}|\phi_l) \quad (9)$$

$$G_{kl} = \frac{1}{2\mu}(\phi_k|p^2|\phi_l) \quad (10)$$

As seen from the above equations, the matrices **B**, $\vec{\mathbf{F}}$, and **G** couple nuclear motion in different electronic states. If we ignore all such coupling we obtain what is usually[6,7] referred to as the Born–Oppenheimer or Born–Oppenheimer adiabatic approximation.

In this article we shall ignore completely the coupling matrix **B**.

We assume next that expansion of the wave function may be terminated after N terms. We let $\phi^i(\vec{x}, R)$ represent an N-dimensional row vector of electronic basis functions of the ith electronic representation. Similarly $\chi^i(\vec{R})$ represents an N-dimensional column vector of nuclear motion wave functions in the ith electronic representation. The total wave function for the system may be written in matrix notation in terms of the ith electronic representation

$$\Psi(\vec{x}, \vec{R}) = \phi^i(\vec{x}, R)\chi^i(\vec{R}) \quad (11)$$

Assume we pick a basis set ϕ^n which is linearly independent but not necessarily orthogonal. The overlap matrix is defined by

$$\mathbf{S} = (\phi^n|\phi^n) \quad (12)$$

where the inner product notation of eq 3a is implied along with conjugate transpose of the vector in the bra and the matrix multiplication. We substitute the total wave function in this nonorthogonal representation into the Schroedinger equation (5) and require the projection of $(H - W)$ onto the N-dimensional space of electronic wave functions be zero to obtain

$$(\phi^n|\frac{1}{2\mu}\vec{p}\cdot\vec{p} + H_{el} - W|\phi^n\chi^n) = 0 \quad (13)$$

Applying the chain rule for differentiation and defining the matrices

$$\mathbf{H}^i = (\phi^i|H_{el}|\phi^i) \quad (14)$$

$$\vec{\mathbf{F}}^i = \frac{1}{2\mu}(\phi^i|\vec{p}|\phi^i) \quad (15)$$

$$\mathbf{G}^i = \frac{1}{2\mu}(\phi^i|p^2|\phi^i) \quad (16)$$

we obtain from eq 13 the following $N \times N$ matrix differential equation for the nuclear motion wave functions

$$\frac{1}{2\mu}\mathbf{S}(p^2\chi^n) + \mathbf{G}^n\chi^n + 2\vec{\mathbf{F}}^n\cdot(\vec{p}\chi^n) + \mathbf{H}^n\chi^n = W\mathbf{S}\chi^n \quad (17)$$

Note that the differential operators are assumed to operate up to the next closing parentheses and no farther.

The presence of the overlap matrix **S** in eq 17 is troublesome. Let **A** be a matrix which transforms the nonorthogonal basis ϕ^n into the orthogonal basis ϕ^o. Then we have

$$\phi^o = \phi^n\mathbf{A} \quad (18)$$

Since the total wave function is invariant to electronic representation we may write

$$\Psi = \phi^o\chi^o \quad (19)$$

where

$$\chi^o = \mathbf{A}^{-1}\chi^n \quad (20)$$

Following the same procedure which led to eq 17 we obtain

$$\frac{1}{2\mu}(p^2\chi^o) + \mathbf{G}^o\chi^o + 2\vec{\mathbf{F}}^o\cdot(\vec{p}\chi^o) + \mathbf{H}^o\chi^o = W\chi^o \quad (21)$$

The method of orthogonalization used in this work corresponds to taking for the matrix **A** the product

$$\mathbf{A} = \mathbf{CU} \quad (22)$$

where

$$\mathbf{C} = \mathbf{S}^{-1/2} \quad (23)$$

and **U** is an arbitrary unitary matrix. In eq 23 the positive square root is implied as discussed by Löwdin.[8] If **U** = **E** (the identity matrix) the method of orthogonalization is known as *symmetric orthogonalization*[8] or sometimes as Löwdin orthogonalization. When symmetric orthogonalization is used the superscript i = o is replaced by i = s. The i = n, o, and s representations will be collectively referred to as diabatic representations to distinguish them from the one to be considered next.

Another choice of **U** is that unitary matrix which diagonalizes the electronic Hamiltonian in the orthogonal basis set. That is we take **U** such that

$$\mathbf{H}^a = \mathbf{U}^\dagger\mathbf{H}^s\mathbf{U} \quad (24)$$

is diagonal. This representation will be called the adiabatic representation.

Since one invariably begins a calculation with a nonorthogonal basis set, it is important to know the following relations

$$\mathbf{H}^\circ = \mathbf{A}^\dagger \mathbf{H}^n \mathbf{A} \tag{25}$$

$$\vec{F}^\circ = \mathbf{A}^\dagger \vec{\mathbf{F}}^n \mathbf{A} + \frac{1}{2\mu} \mathbf{A}^\dagger \mathbf{S}(\vec{p}\mathbf{A}) \tag{26a}$$

$$= \mathbf{A}^\dagger \vec{\mathbf{F}}^n \mathbf{A} + \frac{1}{2\mu} \mathbf{U}^\dagger \mathbf{C}^{-1}(\vec{p}\mathbf{A}) \tag{26b}$$

$$\mathbf{G}^\circ = \mathbf{A}^\dagger \mathbf{G}^n \mathbf{A} + 2\mathbf{A}^\dagger \vec{\mathbf{F}}^n \mathbf{A} \cdot \mathbf{U}^\dagger \mathbf{C}^{-1}(\vec{p}\mathbf{A}) + \frac{1}{2\mu} \mathbf{U}^\dagger \mathbf{C}^{-1}(p^2\mathbf{A}) \tag{27}$$

In deriving eq 26a and 27 we took account of the fact that $\mathbf{A}$ is a function of R and is operated on by $\vec{p}$. We see therefore that given the coupling matrices $\vec{\mathbf{F}}^n$ and $\mathbf{G}^n$ in the original nonorthogonal basis set, the coupling matrices in the orthogonal basis set are given in terms of transformed matrices $\mathbf{A}^\dagger \vec{\mathbf{F}}^n \mathbf{A}$ and $\mathbf{A}^\dagger \mathbf{G}^n \mathbf{A}$ plus additional coupling terms which arise from the dependence of the transformation matrix $\mathbf{A}$ on the internuclear distance.

In this article we shall present calculations (as functions of the internuclear distance) of the matrices $\mathbf{H}^n$, $\mathbf{H}^s$, and $\mathbf{H}^a$. In addition we have calculated the coupling matrices $(1/2\mu)\ \mathbf{U}^\dagger \mathbf{C}^{-1}(\vec{p}\mathbf{A})$ and $(1/2\mu)\ \mathbf{U}^\dagger \mathbf{C}^{-1}(p^2\mathbf{A})$. The matrices $\vec{\mathbf{F}}^n$ and $\mathbf{G}^n$ were not obtained.

III. Model Effective Potentials

We assume the hydrides under consideration may be treated as two-electron systems. The model Hamiltonian at internuclear distance R is assumed to be[5]

$$H_{el}(R) = \tfrac{1}{2}p_{x_1}^2 + \tfrac{1}{2}p_{x_2}^2 - \frac{1}{x_{1H}} - \frac{1}{x_{2H}} - \frac{Z_c}{x_{1M}} - \frac{Z_c}{x_{2M}} + V_M(x_{1M}) + V_M(x_{2M}) + \frac{1}{|\vec{x}_1 - \vec{x}_2|} + \frac{Z_c}{R} \tag{28}$$

where x_{iH} and x_{iM} are the distances of electron i from the proton and the core M^+ (M = Na, K, or Mg^+; $M^+ = Na^+$, K^+, or Mg^{2+}), respectively, Z_c is the net charge on the core, and both electrons are assumed to interact with the core through the Coulomb potential and a model effective potential V_M. Both electrons, independent of their angular momenta about the core, are assumed to interact with the core through the same effective potential. This is an important simplification as compared to the ab initio effective potentials used elsewhere.[9] The effective potential chosen, in all cases, is the ground s-state effective potential. We shall see that, although this approximation in our model is certainly a source of inaccuracy, atomic energies calculated in this manner are in excellent agreement with the experimental values.

The concept of an effective potential is quite old and was developed independently by Hellmann[10] and Gombas.[11] Two recent review articles are available.[12] We approximate the effective potential V_M in eq 28 by the Hellmann potential

$$V_H(x_{iM}) = A x_{iM}^{-1} \exp(-\kappa x_{iM}) \tag{29}$$

where the parameters A and κ are to be determined empirically. The parameters have been determined in different ways by different workers. To compare how well some of these different effective potentials represent the actual energy levels of the valence electron, we have used a finite difference method[13] for numerical determination of eigenvalues to compute the first five s-state and p-state energies for potassium for four different effective potentials. We have used the s-state effective potential in each case and obtained the p-state energies by adding the appropriate centrifugal potential to the effective potential. The results are given in Table I. In that table E_H, E_{HG}, and E_S denote the energies obtained using the effective potentials of Hellmann as quoted by Szasz and McGinn,[14] of Hart and Goodfriend,[15] and of Schwarz,[16-18] respectively. For comparison, the table also includes experimental values[19] E_{expt} and energies E_{SM} obtained using the Philips–Kleinman effective potential[20] as calculated by Szasz and McGinn.[21]

TABLE I: Experimental and Calculated Energies for Potassium Using Various Effective Potentials

State	E_{expt}, eV	E_H, eV	E_{HG}, eV	E_{SM}, eV	E_S, eV
4s	−4.431	−5.173	−4.776	−3.984	−4.343
5s	−1.734	−2.033	−1.949	−1.718	−1.765
6s	−0.937	−1.062	−1.032	−0.942	−0.953
7s	−0.587	−0.650	−0.635	−0.592	−0.596
8s	−0.402	−0.438	−0.430	−0.405	−0.407
4p	−2.726	−2.894	−2.775	−2.615	−2.848
5p	−1.276	−1.352	−1.317	−1.253	−1.327
6p	−0.744	−0.781	−0.766	−0.736	−0.768
7p	−0.488	−0.508	−0.500	−0.484	−0.501
8p	−0.345	−0.356	−0.351	−0.341	−0.351
Φ[a]	0.000	0.697	0.182	0.213	0.027

[a] Sum of squares of the differences of experimental and calculated energies, eq 30.

As a measure of how well these effective potentials represent the actual states of the atom, we have calculated the sum of the squares of the differences of the experimental and calculated energies

$$\Phi = \Sigma(E_{expt} - E_{calcd})^2 \tag{30}$$

where the sum is extended over the ten states considered and we have entered the result in the last row of Table I. The effective potential due to Schwarz gives the best overall agreement with experiment in this case and we have adopted Schwarz's effective potentials for use in our model Hamiltonian, eq 28. The values of the parameters A and κ are listed in Table II. Note that in ref 16 an incorrect value is quoted for Mg^+. The correct value listed in Table II is given in later references.[17,18]

Since the s-state effective potentials give good approximations for the p-state energies for potassium, the angular momentum dependence is in some sense weak, and our use of s-state potentials only is partly justified. Below we shall see that this statement is also true for the atomic states of interest for Na and Mg^+.

The effective potential obtained by Callaway and Laghos[22] for Na by a different method is very similar to the effective potential of Schwarz for Na.

IV. Calculations

One-Electron Atomic Basis Set. All atomic basis functions in this work are linear combinations of Slater-type orbitals[23] (STO's) with principal quantum numbers n_k and orbital exponents ζ_k.

TABLE II: Pseudopotential Parameters in Hartree Atomic Units for the S State Pseudopotentials for Na, K, and Mg^+

Atom	Z_c	A	κ
Na	1.0	14.0	2.267
K	1.0	18.0	1.866
Mg^+	2.0	30.0	2.855

We have chosen for the H^- wave function the GF function due to Goddard.[24] We have used the function involving four STO's as given in Table IV of ref 24.

For each covalent configuration, we use a hydrogen 1s orbital centered on the hydrogen atom and a pseudowave function centered on the alkali atom, in particular the pseudowave function for the atomic state which gives rise to the molecular state of interest. Three covalent configurations (corresponding to the two lowest s states and the lowest p state of the alkali) were included and the pseudowave functions for these states were obtained in the following way. To obtain a set of STO's in which to expand the pseudowave function, we first of all included the STO's given by Schwarz[17] for the ground and first excited s states and for the lowest p state. We also included the two most important STO's in the pseudowave functions given by Szasz and McGinn.[21] Using this set of STO's the secular equation was calculated using the effective Hamiltonian

$$H_M = \tfrac{1}{2}p_{x_1}^2 - \frac{Z_c}{x_{1M}} + V_M \qquad (31)$$

where V_M is approximated by eq 29 with the parameters given in Table II. The results are given in Table III where the calculated atomic energies are compared with the experimental values. The agreement between calculated and experimental atomic energies is especially good for neutral cases. We therefore have further verification that the effective potential is independent enough of angular momentum that one effective potential may be used for all the states.

Since the avoided crossings considered later in this article occur at rather large internuclear separation (e.g., as large as 23 a_0 in Na and 28 a_0 in K), it is important to check the behavior of our pseudowave functions at large distance from the nucleus. Comparison of numerical Hartree–Fock functions for potassium calculated with the program of Froese-Fischer[25] and coulomb approximation[26] functions indicates that in the regions of interest corresponding to the occurrence of avoided crossings (see below for the exact positions of these avoided crossings) the coulomb approximation functions give the correct behavior except possibly for normalization. Comparison of the logarithms of our wave functions with those of the coulomb approximation wave functions indicates that for Na and K, the wave functions are fairly good at distances less than about 14 or 15 a_0 while we may expect that the ground state wave functions are too large at larger distances. However, we will show below that the diabatic matrix elements H_{2j}^n (j = 1, 3, 4) involving the nonorthogonal covalent configurations of NaH and KH which dissociate to ground atomic states are small for $x > 9$ a_0. Thus the wave functions do not need to be accurate to as large a distance for the ground state as for the excited states. For the excited states of Na and K, the wave functions appear to be more accurate at large distances but must eventually, at large enough distances, become too small. For Mg^+ the wave functions may be in serious error even for distances as small as 8 a_0. In this case, however, the important curve crossings occur at smaller distances [less than 6 a_0 for the covalent state which dissociates to Mg^+ (3p) and about 10 a_0 for the covalent state which dissociates to Mg^+ (4s)] and thus accuracy is not needed at distances as large as for the neutral cases. Nevertheless, we will show below that the coupling matrices in the MgH^+ system may have elements which are large at distances as great as about 14 a_0. Therefore, the quantitative results for MgH^+ may need to be reexamined and should not be treated with as much confidence as the results for NaH and KH.

TABLE III: Experimental and Calculated Energies in Hartree Atomic Units at Infinite Internuclear Separation for the Four Atomic Configurations Used in Determining the Molecular Basis Set

State	E_{expt}[a]	E_{calcd}[a]	ΔE[b]
Na(3s) + H(1s)	−0.68882	−0.68886	0.00004
Na(3p) + H(1s)	−0.61152	−0.61189	0.00037
Na(4s) + H(1s)	−0.57222	−0.57154	−0.00068
$Na^+ + H^-$	−0.52775	−0.51359	−0.01416
K(4s) + H(1s)	−0.65952	−0.65948	−0.00004
K(4p) + H(1s)	−0.60018	−0.60459	0.00442
K(5s) + H(1s)	−0.56371	−0.56483	0.00112
$K^+ + H^-$	−0.52775	−0.51359	−0.01416
Mg^+(3s) + H(1s)	−1.05254	−1.04963	−0.00291
Mg^+(3p) + H(1s)	−0.88974	−0.88529	−0.00445
Mg^+(4s) + H(1s)	−0.73448	−0.73563	0.00115
$Mg^{2+} + H^-$	−0.52775[c]	−0.51359	−0.01416

[a] The zero of energy is for $M^+ + H^+ + 2e^-$ where M is Na, K, or Mg^+. [b] The amount by which the calculated energy differs from the experimental one. [c] The energy of $Mg(3s^2) + H^+$ is −0.83346 hartree; although this is lower than $Mg^{2+} + H^-$, this state does not have a long-range coulomb attraction and may be less important for causing interactions among the covalent diabatic states.

Two-Electron Nonorthogonal Molecular Basis Set. Using the one-electron atomic basis functions ψ_i described above, we form two-electron valence bond wave functions as follows

$$\phi_m^n(\vec{x}_1, \vec{x}_2, R) = N_m(R)[\psi_i(1)\psi_j(2) \pm \psi_j(1)\psi_i(2)] \times (1/\sqrt{2})[\alpha(1)\beta(2) \mp \beta(1)\alpha(2)] \qquad (32)$$

where the normalization constant is

$$N_m(R) = [2(1 + s_{ij}^2)]^{-1/2} \qquad (33)$$

and the overlap between atomic functions is

$$s_{ij} = (\psi_i | \psi_j) \qquad (34)$$

The numbers in parentheses indicate whether the ψ_i are to be taken as functions of the vector to electron 1 or electron 2 from the nucleus on which the atomic basis function is centered. The functions $\alpha(i)$ and $\beta(i)$ are the usual spin functions for electron i, and the upper and lower signs in eq 32 correspond to the singlet and triplet states, respectively.

For the ionic configuration, ψ_i and ψ_j are the GF orbitals for H^- (see above). For the covalent configurations, ψ_j is always the 1s orbital of H while ψ_i is the orbital corresponding to the atomic valence state at infinite internu-

clear separation which gives rise to the molecular state of interest. From the ground and first excited atomic s states, we obtain $^1\Sigma^+$ and $^3\Sigma^+$ molecular states. From the first atomic p state, we obtain $^1\Sigma^+$ and $^3\Sigma^+$ molecular states with $m_l = 0$ STO's while $^1\Pi$ and $^3\Pi$ states are obtained with $m_l = \pm 1$ STO's. From the ionic configuration, we obtain only the $^1\Sigma^+$ state since the bound state of H^- is a singlet.

Since the diagonal matrix elements of the electronic Hamiltonian in the diabatic representations will cross each other as the internuclear distance changes, we need to adopt a numbering convention for the molecular states which shall be used at all values of the internuclear distance. Within the set of $^1\Sigma^+$ diabatic molecular states, we shall always assign the number 1 to the molecular state arising from the ionic configuration and label it 1 $^1\Sigma^+$, the number 2 to the molecular state arising from the ground atomic state and label it 2 $^1\Sigma^+$, the number 3 to the molecular state arising from the atomic p state and label it 3 $^1\Sigma^+$, and the number 4 to the molecular state arising from the excited atomic s state and label it 4 $^1\Sigma^+$. Within the set of $^3\Sigma^+$ molecular states, there is no molecular state arising from the ionic configuration, so we number the molecular states in the same order as the atomic states from which they originate. To emphasize the physical character of the covalent $^{1,3}\Sigma^+$ states we will also use the notation ns $^{1,3}\Sigma^+$, np $^{1,3}\Sigma^+$, and n*s $^{1,3}\Sigma^+$ where n is the principal quantum number of the valence electron in the ground state and $n^* = n + 1$. No numbering scheme is needed for the Π states since only one singlet and one triplet are considered for each value of m_l.

In the adiabatic representation, no crossing of curves occurs and we number them at each value of R in the order of their increasing energies. Following the usual spectroscopic notation, we may also refer to the adiabatic states as $X^1\Sigma^+$, $A^1\Sigma^+$, $B^1\Sigma^+$, and $C^1\Sigma^+$ for the singlets in order of increasing energy and $a^3\Sigma^+$, $b^3\Sigma^+$, and $c^3\Sigma^+$ for the triplets again in order of increasing energy. The Π states will be referred to as simply $^1\Pi$ and $^3\Pi$ since there is only one of each and they are the same in all representations.

Using the model electronic Hamiltonian (28) with the Hellmann effective potentials due to Schwarz and the molecular functions (32), we have calculated the electronic Hamiltonian matrix elements defined by eq 14 with $i = n$ as functions of the internuclear distance.

All the necessary molecular integrals were evaluated using a program due to Schaeffer.[27] This program has the advantage that integrals are computed directly over atomic orbitals rather than over atomic basis functions.

The experimental atomic energies of Table III represent the asymptotic limits which the diagonal elements of the electronic Hamiltonian should approach at infinite internuclear separation in each of the nonorthogonal diabatic, orthogonal diabatic, and adiabatic representations where the zero of energy is set at $M^+ + H^+ + 2e^-$ with M = Na, K, or Mg^+. The error involved in our calculation is given by the energy ΔE_k for each atomic state k and we see that this error is not the same for different atomic states. We could make one of the diagonal matrix elements approach the correct asymptotic value by a simple change in the zero of energy which in a nonorthogonal representation amounts to adding the quantity $\Delta E_k S_{ij}$ to each element $H_{ij}{}^n$ of the Hamiltonian matrix where ΔE_k is the amount by which the zero is changed and S_{ij} is the overlap between the states i and j. Since the error ΔE_k is not the same for all states, however, the other matrix elements would still have the wrong large R asymptotic values.

To make all the diagonal elements have the correct asymptotic energies, we have added to each diagonal element $H_{kk}{}^n$ of the Hamiltonian matrix in the nonorthogonal diabatic representation the quantity ΔE_k listed in Table III. In making this correction, we have assumed that the error involved in our calculation is independent of internuclear distance in a given nonorthogonal diabatic valence-bond configuration, which is of course not true, but we believe that this method is a reasonable way of adjusting the curves to the correct asymptotic values especially since the corrections involved are small. One of the reasons we preferred the Schwarz effective potentials to other choices is that the ΔE_k are so small for this case.

The off-diagonal matrix elements in a nonorthogonal representation should also be adjusted whenever the diagonal matrix elements are altered as mentioned above. However, in this case we have not added the same value to all the diagonal matrix elements, and therefore there is no unique method for adjusting the off-diagonal matrix elements. Therefore no adjustment of the off-diagonal matrix elements has been made.

After addition of the quantities ΔE_k to the diagonal matrix elements, the zero of energy was adjusted to correspond to the ground state atomic configuration for each system by adding the quantity $|E_1|S_{ij}$ to each matrix element where $|E_1|$ is the absolute value of the experimental energy of the ground state of M + H where M = Na, K, or Mg^+ as listed in Table III.

By adjusting the diagonal matrix elements before rather than after orthogonalization, we ensure that the final adiabatic potential energy curves obtained are independent of the method of orthogonalization.

Our four-state molecular valence-bond basis set for the $^1\Sigma^+$ states does not take into account the large polarization of H^- by the core M^+ as well as the smaller polarization of the core M^+ by H^-. We include this aspect of the system in our model by adding a polarization potential V_p to the calculated matrix element $H_{11}{}^n$ corresponding to the ionic configuration. The polarization potential chosen is given by[5]

$$V_p = -\frac{\alpha_+ + \alpha_-}{2R^4}\left\{1 - \exp\left[-\left(\frac{R}{\gamma}\right)^6\right]\right\} \qquad (35)$$

where α_+ is the dipole polarizability of the core M^+ and α_- is the dipole polarizability of H^-.

The parameter γ is adjustable. It was determined in such a way that after orthogonalization of the basis functions and diagonalization of the Hamiltonian matrix in the orthogonal basis, the adiabatic curves for the A states have dissociation energies as close as possible to the experimental values. This variation of γ could be carried out with little effect on the X and C state curves but with considerable effect on the A and B state curves. The polarization potential, of course, has no effect on the $^3\Sigma^+$, $^1\Pi$, or $^3\Pi$ states. We shall see below that the final A state curves obtained in this way give fairly good agreement with experimentally determined RKR curves although the curves for KH and MgH^+ are displaced to larger values of R than the respective experimental ones. The final values of γ used in this work are 9.3 a_0 for NaH, 9.9 a_0 for KH, and 5.7 a_0 for MgH^+. The dipole polarizabilities were taken from the tabulation of Dalgarno.[28]

For later computational purposes we have fit the ele-

ments of the electronic Hamiltonian matrix in the nonorthogonal diabatic basis to analytical forms containing three to five linear parameters and two or three nonlinear parameters adjusted to give the best fit in a least-squares sense to the calculated points. All curve fitting was done using the Marquardt non-linear least-squares method.[29] The analytic forms and curve fits are given elsewhere.[30]

Orthogonal Diabatic Basis. Using the orthogonalization procedure described above, we have transformed the electronic Hamiltonian matrix in the nonorthogonal diabatic basis to the symmetrically orthogonalized basis. In the case of the $^1\Sigma^+$ states we have included the correction of eq 35.

The matrix elements for the transformation $\mathbf{C} = \mathbf{S}^{-1/2}$ from the nonorthogonal to the orthogonal diabatic basis were also fit to an analytic form for later computational purposes. The form used and the parameters of the fits are given elsewhere.[30]

The fits for $\mathbf{C}(R)$ and $\mathbf{H}^n(R)$ will also be used below to determine the values of R_e and D_e for the adiabatic potential curves, to determine the crossing points in both the nonorthogonal and orthogonal diabatic representations, and to calculate the coupling matrices between adiabatic states and to generate points for plots of the elements of these matrices.

It is interesting to note that the elements of the transformation matrix $\mathbf{C}(R)$ are quite smoothly varying functions of R. This behavior might have been expected since the method of symmetric orthogonalization is, in a certain sense, a gentle procedure which produces a minimum change in the basis set. At small values of R, however, the difficulty of orthogonalization increases and rather large amounts of the nonorthogonal basis functions are added and subtracted to maintain orthogonality. As the two atoms approach each other, the off-diagonal elements of the overlap matrix become large, some of the basis functions become almost linearly dependent, and one of the eigenvalues of the overlap matrix becomes very small. Thus, the norm of $\mathbf{C}$ becomes very large.

Adiabatic Potential Curves and Electronic Eigenfunctions. Diagonalization of the Hamiltonian matrix in the symmetrically orthogonalized diabatic basis yields the adiabatic potential energy curves $H_{ii}^a(R)$ according to eq 24. We recall from eq 22 that the matrix $\mathbf{A}$ is defined in terms of the unitary matrix $\mathbf{U}$ which diagonalizes the electronic Hamiltonian in the symmetrically orthogonalized diabatic basis. Therefore, the columns of the matrix $\mathbf{U}$ are the eigenvectors of the matrix $\mathbf{H}^s$, and since the negative of an eigenvector is still an eigenvector with the same eigenvalue, a problem arises in establishing the sign to be given to these eigenvectors. To calculate the coupling matrices defined in eq 26 and 27 we must take derivatives of the elements of the matrix $\mathbf{U}$ and therefore we must establish a sign convention which yields smoothly varying functions of R. In the case of avoided crossings as considered here, the character of the eigenvectors changes rapidly over very small distances and the relative contributions of the components change rapidly also.

To overcome this difficulty we have adopted the following procedure. At large internuclear distances, beyond the position of the last crossing of ionic and covalent curves, the character of each adiabatic curve is unambiguous and corresponds to a configuration chosen as one of the original basis functions. We start the calculation of $\mathbf{U}$ at some value $R = R_n$ where the sign of each column is determined and proceed stepwise to smaller values R_{n-1}, R_{n-2}, etc. At each point after the first, the calculated elements of column i of the matrix $\mathbf{U}$ are compared to the values at the previous point by computing the two quantities

$$\lambda_\pm = \sum_{k=1}^{N} [U_{ki}(R_n) \pm U_{ki}(R_{n-1})]^2 \tag{36}$$

for each column of $\mathbf{U}$. If the minimum of these two quantities is equal to λ_-, then the sign of column i is left unchanged while if the minimum is equal to λ_+, the sign of column i is changed to its negative. Thus, the decision for the sign of the eigenvectors is based on a smoothness criterion involving all the components of the vector at each value of R.

This procedure was carried out with step size $R_n - R_{n-1} = 0.1a_0$. It yields continuous, although sometimes sharply varying, functions. We checked that the results obtained are independent of step size.

Coupling Matrices in the Adiabatic Representation. Note that $\mathbf{A}$ is a function only of R (not of $\vec{R}$) so that the partial derivative operator $\tilde{p}$ reduces to an ordinary derivative with respect to R in eq 26b and 27. Defining

$$\mathbf{M} = \frac{1}{2\mu}\mathbf{U}^\dagger\mathbf{C}^{-1}\frac{d\mathbf{A}}{dR} \tag{37}$$

$$\mathbf{M}_1 = \frac{1}{2\mu}\mathbf{U}^\dagger\mathbf{C}^{-1}\left(\frac{d\mathbf{C}}{dR}\right)\mathbf{U} \tag{38}$$

$$\mathbf{M}_2 = \frac{1}{2\mu}\mathbf{U}^\dagger\frac{d\mathbf{U}}{dR} \tag{39}$$

and using eq 22 we may write

$$\frac{1}{2\mu}\mathbf{U}\mathbf{C}^{-1}(\tilde{p}\mathbf{A}) = -i\mathbf{M}\hat{e}_R = -i(\mathbf{M}_1 + \mathbf{M}_2)\hat{e}_R \tag{40}$$

where $\hat{e}_R$ is a unit vector in the direction of $\vec{R}$. Similarly we define the matrices

$$\mathbf{N} = \frac{1}{2\mu}\mathbf{U}^\dagger\mathbf{C}^{-1}d^2\mathbf{A}/dR^2 \tag{41}$$

$$\mathbf{N}_1 = \frac{1}{2\mu}\mathbf{U}^\dagger\mathbf{C}^{-1}(d^2\mathbf{C}/dR^2)\mathbf{U} \tag{42}$$

$$\mathbf{N}_2 = \frac{1}{2\mu}\mathbf{U}^\dagger\, d^2\mathbf{U}/dR^2 \tag{43}$$

so that

$$\frac{1}{2\mu}\mathbf{U}^\dagger\mathbf{C}^{-1}(\tilde{p}^2\mathbf{A}) = -\mathbf{N} = -(\mathbf{N}_1 + 4\mu\mathbf{M}_1\mathbf{M}_2 + \mathbf{N}_2) \tag{44}$$

From the above definitions, we see that the matrices $\mathbf{M}_1$ and $\mathbf{N}_1$ represent contributions to the coupling matrices which arise primarily from the orthogonalization procedure while the matrices $\mathbf{M}_2$ and $\mathbf{N}_2$ represent contributions which arise from the diagonalization procedure. We may thus separate the effects of the two procedures and analyze the relative contribution of each to the total coupling matrices.

The curve fits to $\mathbf{H}^n(R)$, $V_p(R)$, and $\mathbf{C}(R)$ are used to generate $\mathbf{A}$, $\mathbf{C}$, and $\mathbf{U}$ at four equally spaced points $10^{-3}\ a_0$ apart. Then the required first and second derivatives of $\mathbf{A}$, $\mathbf{C}$, and $\mathbf{U}$ are calculated using a four-point difference formula.

V. Results and Discussion

Nonorthogonal Diabatic Basis. The calculated Hamiltonian matrix elements in the nonorthogonal diabatic representation for the $^1\Sigma^+$ valence-bond states are shown in Fig-

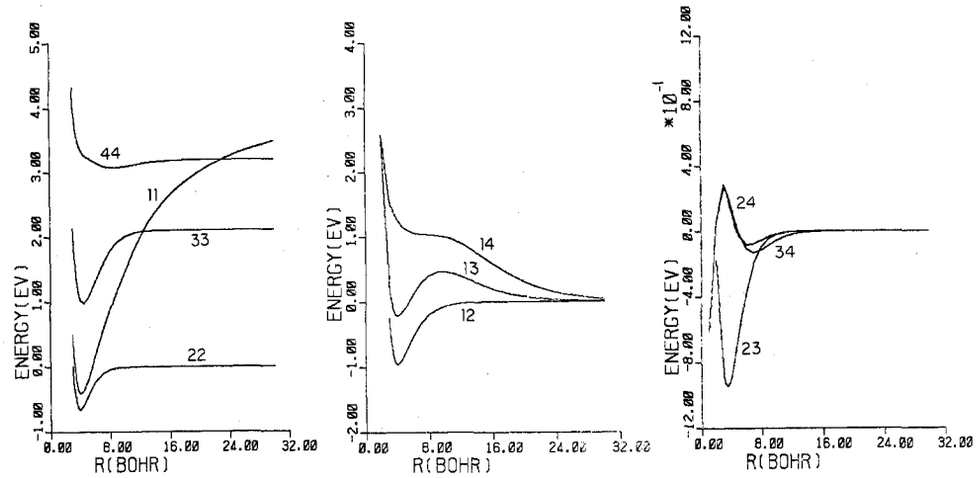

Figure 1. The matrix elements H_{ij}^n for the $^1\Sigma^+$ states of NaH in the nonorthogonal diabatic basis as functions of the internuclear distance R. Each curve is labeled by the pair of indices ij. The curve corresponding to H_{11}^n includes the polarization correction of eq 35. The notation on the right-most ordinate means that each number along the ordinate should be multiplied by 10^{-1}.

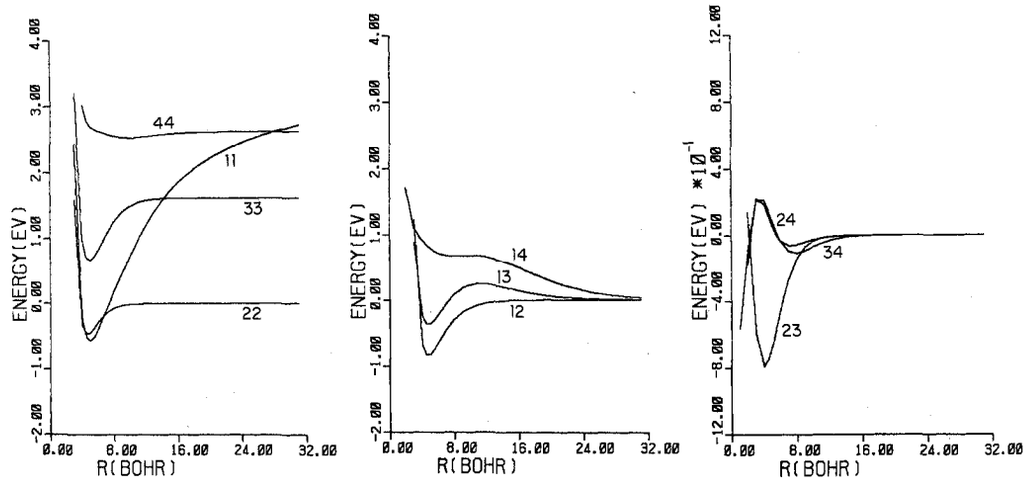

Figure 2. Same as Figure 1 except for KH.

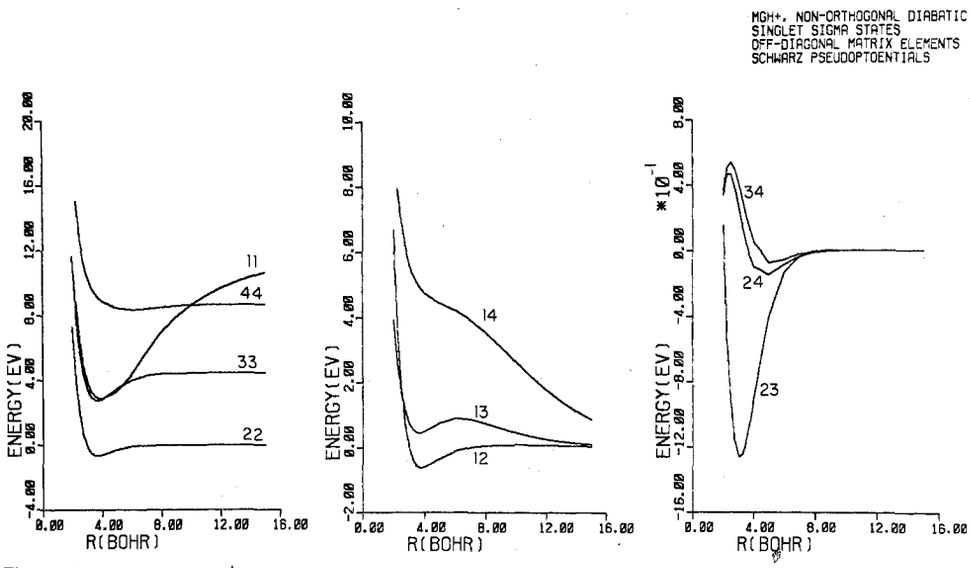

Figure 3. Same as Figure 1 except for MgH^+.

ure 1 for NaH, Figure 2 for KH, and Figure 3 for MgH^+. The curves corresponding to the matrix elements H_{11}^n in each case include the polarization potential correction of eq 35 and the reader should henceforth assume this polarization potential is present.

We note first of all the occurrence of curve crossings be-

tween the ionic curve H_{11}^{n} and the covalent curves. It is particularly interesting that no crossing occurs for NaH between H_{11}^{n} and the lowest covalent curve H_{22}^{n}. In earlier treatments of the problem it was assumed that a crossing would occur at a large value of R (7.7 a_0 by Bates and Boyd[3] and 7.55 a_0 by Grice and Herschbach[4]) where H_{22}^{n} was assumed to be essentially constant and where H_{11}^{n} was assumed to be well represented by the sum of a coulomb potential and a polarization potential. However, Figure 1 shows that the above assumption fails for our calculations and no crossing occurs because our calculated H_{11}^{n} is sufficiently less attractive than previous workers assumed. This same effect is true for KH where the crossing of the ionic curve with the lowest covalent curve is found at smaller R values than those assumed by Bates and Boyd[3] and by Grice and Herschbach.[4] There is no crossing between the ionic and lowest covalent states for MgH^+ either, but in this case the absence of the crossing is due to the higher ionization potential of Mg^+ and no crossing was expected.

We next note the large separation in distance between the attractive regions of the ionic curve H_{11}^{n} and the covalent curve H_{33}^{n} for NaH and KH. Configuration interaction including these two states yields the qualitative features of the adiabatic $A^1\Sigma^+$ state potential curve with the abnormally broad, flat minimum which leads to the well-known spectroscopic anomalies[31,32] in these states. It is easy to see here that this effect is due to the fact that the ionic curve H_{11}^{n} is the second lowest curve in this region and that its attractive region occurs at abnormally large distances, i.e., around $R = 9\ a_0$. The effect is missing for MgH^+ since the two curves H_{11}^{n} H_{33}^{n} essentially coincide near their minima so no extended well region is expected for the A state. The A state for MgH^+ has been observed to be normal spectroscopically.[33]

The similarity of the off-diagonal Hamiltonian matrix elements for all three molecules is striking. We note in particular the long-range nature of the matrix elements H_{12}^{n}, H_{13}^{n}, and especially H_{14}^{n} which are the interactions of the ionic state with the covalent states. The matrix elements H_{23}^{n}, H_{24}^{n}, and H_{34}^{n} between covalent states are of shorter range. It is interesting that the matrix element H_{24}^{n} between the $ns\ ^1\Sigma^+$ and $n^*s\ ^1\Sigma^+$ is very similar to the matrix element H_{34}^{n} between the $np\ ^1\Sigma^+$ and $n^*s\ ^1\Sigma^+$ states while the matrix element H_{23}^{n} between the $ns\ ^1\Sigma^+$ and $np\ ^1\Sigma^+$ states is quite different.

The Hamiltonian matrix elements for the $^3\Sigma^+$ valence bond states are shown in Figure 4 for NaH, Figure 5 for KH, and Figure 6 for MgH^+. All diagonal matrix elements correspond to covalent configurations for this symmetry. Although not shown on the figures, curve crossings occur between the matrix element H_{11}^{n} and the two higher matrix elements H_{22}^{n} and H_{33}^{n} at small values of R. These crossings will produce rather large coupling matrices in these regions which will be discussed below.

The off-diagonal matrix elements are again very similar from one molecule to another. The matrix elements H_{13}^{n} and H_{23}^{n} between the $n^*s\ ^3\Sigma^+$ state and the $ns\ ^3\Sigma^+$ and $np\ ^3\Sigma^+$ states, respectively, are again similar to each other while the element H_{12}^{n} between the $ns\ ^3\Sigma^+$ and $np\ ^3\Sigma^+$ states is quite different.

Orthogonal Diabatic Basis. The Hamiltonian matrix elements in the orthogonal diabatic representation for the $^1\Sigma^+$ states are shown in Figure 7 for NaH, Figure 8 for KH, and Figure A1[34] for MgH^+. Comparing these curves with the curves in the nonorthogonal representation we note a number of differences. The attractive wells for the $3^1\Sigma^+$ and $4^1\Sigma^+$ states of NaH and KH are not as deep as they were in the nonorthogonal basis and the well for the $2^1\Sigma^+$ state has completely disappeared. The $2^1\Sigma^+$ and $3^1\Sigma^+$ states of MgH^+ have wells which are not quite as deep as in the nonorthogonal basis while the $4^1\Sigma^+$ state has a slightly deeper well than in the nonorthogonal basis. The curve corresponding to the ionic configuration H_{11}^{s} (R) has shifted position relative to the other diagonal elements thereby

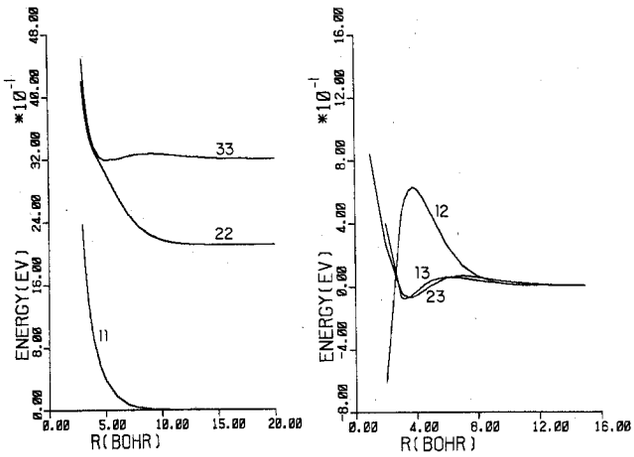

Figure 4. The matrix elements H_{ij}^{n} for the $^3\Sigma^+$ states of NaH in the nonorthogonal diabatic basis as functions of internuclear distance R. Each curve is labeled by the pair of indices ij.

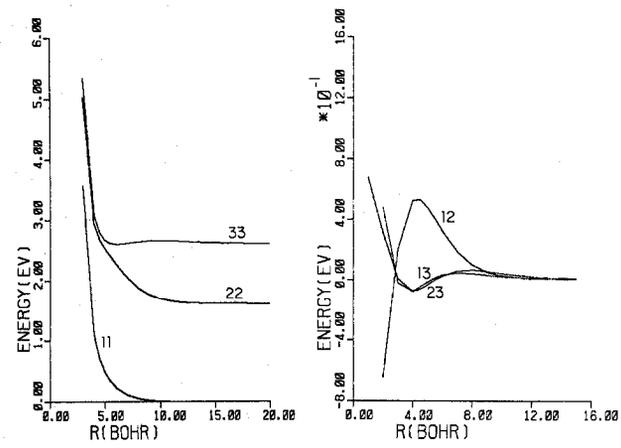

Figure 5. Same as Figure 4 except for KH.

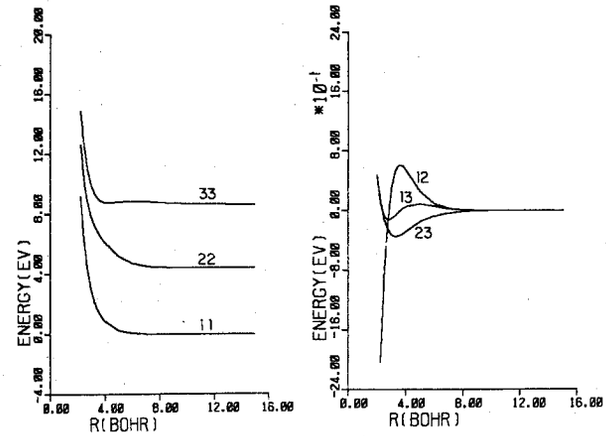

Figure 6. Same as Figure 4 except for MgH^+.

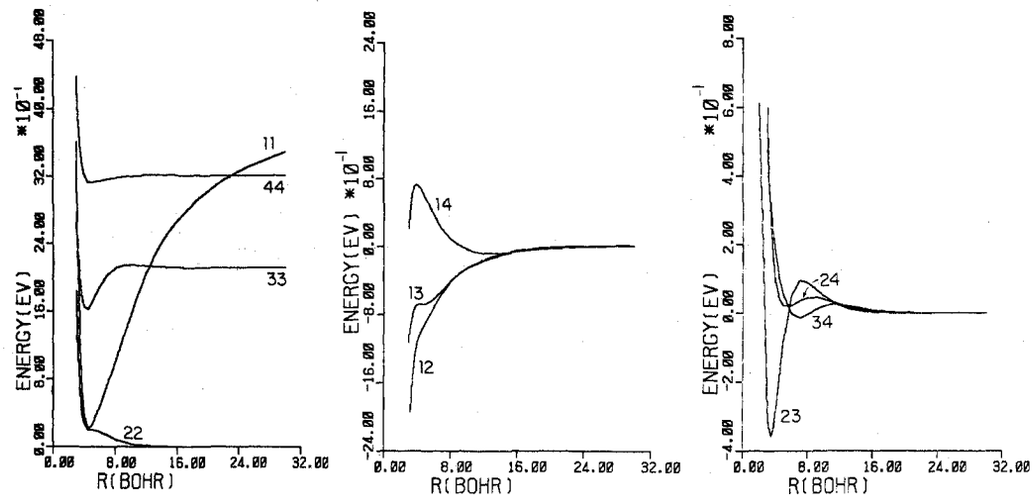

Figure 7. The matrix elements H_{ij}^s for the $^1\Sigma^+$ states of NaH in the symmetrically orthogonalized diabatic basis as functions of internuclear distance R. Each curve is labeled by the pair of indices ij.

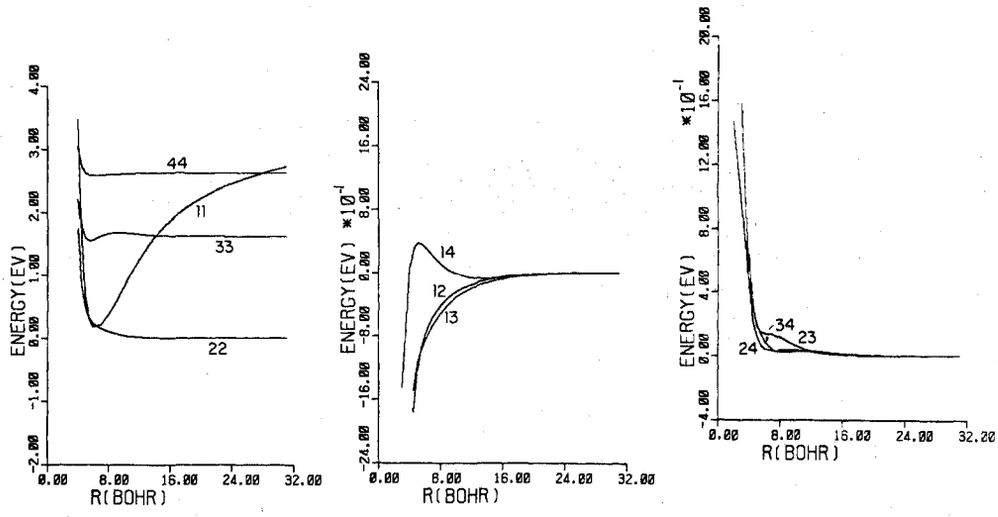

Figure 8. Same as Figure 7 except for KH.

changing the positions of the crossing points and in fact introducing new crossing points. New crossing points at small R values appear for all three molecules; in the case of NaH, where there was no crossing between the $1^1\Sigma^+$ and $2^1\Sigma^+$ potential curves in the nonorthogonal basis, there are now two crossings between $R = 4\ a_0$ and $R = 5\ a_0$. In the case of MgH^+, the ionic curve no longer so closely resembles the potential curve of the $3^1\Sigma^+$ state near its minimum.

The off-diagonal Hamiltonian matrix elements have also changed considerably. Nevertheless, the corresponding matrix elements are still remarkably similar from molecule to molecule, the most notable exception being the matrix element H_{23}^s of KH which is somewhat different from the same matrix element for NaH or MgH^+. It is interesting that the matrix elements H_{12}^s, H_{13}^s, and H_{14}^s between the ionic configuration and the covalent configurations are not of as long a range as they were in the nonorthogonal representation.

Mulliken,[31] neglecting overlap, has reported a calculation for the diabatic matrix element between the lowest covalent state and the ionic state in LiH. His result, as a function of R, has the same qualitative shape as the matrix elements $H_{12}^s(R)$ reported here. His function varies from -1.5 eV at $R = 2.0\ a_0$ to -0.1 eV at $R = 5\ a_0$ while the functions reported here vary from -11.6 to 0.9 eV for NaH, from -21.6 to -1.2 eV for KH, and from -5.0 to -1.0 eV for MgH^+ over the same interval.

The Hamiltonian matrix elements for the $^3\Sigma^+$ states in the symmetrically orthogonalized representation are shown in Figure 9 for NaH, Figure 10 for KH, and Figure A2[34] for MgH^+. The most interesting difference between the two representations is the introduction of additional curve crossings of the diagonal matrix elements at small values of R. These crossings will show up in the coupling matrices discussed below. The off-diagonal matrix elements have changed shape but the similarity noticed in the nonorthogonal representation between the elements H_{13}^n and H_{23}^n remains for H_{13}^s and H_{23}^s while the element H_{12}^s has a different character.

The shapes of these matrix elements as functions of R depend on the particular method of orthogonalization chosen. Since we are free to multiply our orthogonalizing matrix by an arbitrary unitary matrix as discussed above, it is possible to produce matrix elements in an orthogonal diabatic representation with widely varying characteristics. We have carried out the calculation for canonical orthogonalization[8] and have found qualitative and quantitative differences in all the matrix elements. For example, for NaH

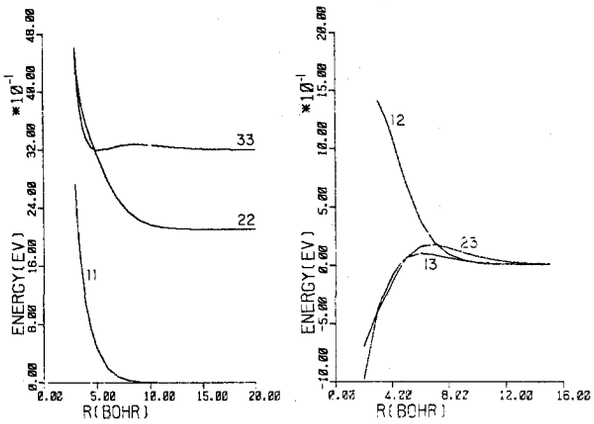

Figure 9. The matrix elements H_{ij}s for the $^3\Sigma^+$ states of NaH in the symmetrically orthogonalized diabatic basis as functions of internuclear distance R. Each curve is labeled by the pair of indices ij.

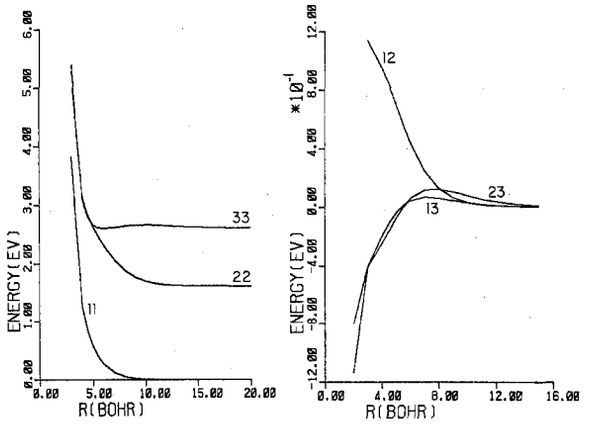

Figure 10. Same as Figure 9 except for KH.

the matrix element H_{12} at 5 a_0 is −0.903 eV for symmetric orthogonalization and 0.392 eV for canonical orthogonalization, the matrix element H_{13} at 12 a_0 is −0.176 and −0.410 eV, respectively, and the matrix element H_{14} at 20 a_0 is −0.035 and 0.034 eV, respectively.

As discussed by O'Malley,[35] however, some diabatic representations have particular physical significance. In the work presented here, the original nonorthogonal valence bond molecular basis has particular significance in terms of the bonding models which have been used previously to discuss the interaction of ionic and covalent configurations in the hydrides considered here. Symmetric orthogonalization was then chosen because it gives an orthogonal basis which differs from the physically motivated basis as little as possible.

The Adiabatic Potential Curves and Electronic Eigenfunctions. We present now the results for the adiabatic potential curves. The results are shown for NaH in Figure 11, for KH in Figure 12, and for MgH^+ in Figure 13.

We recall that the parameter γ in the polarization potential was adjusted in such a way that the experimental value of the dissociation energy of the $A^1\Sigma^+$ states was not exceeded. Comparing the $A^1\Sigma^+$ states obtained in this way with the experimentally determined RKR potential curves which are discussed in ref 30 and shown in Figures 11–13, we see that our procedure for determining γ yields adiabatic $A^1\Sigma^+$ potential energy curves which have the correct shape but which are shifted to larger values of R especially in the cases of KH and MgH^+.

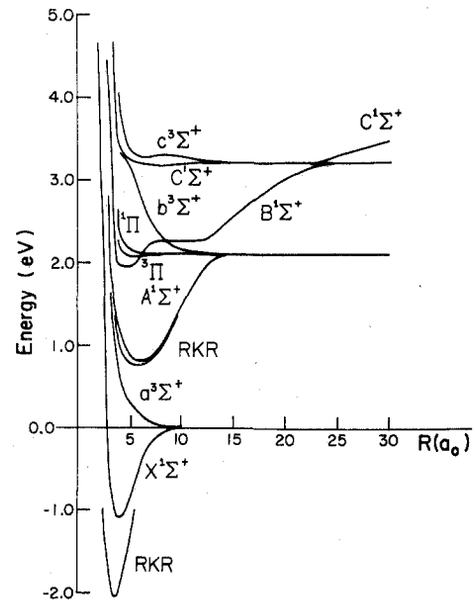

Figure 11. The adiabatic potential curves for NaH. All nine curves calculated in this work are shown plus the experimentally determined RKR curves for the $X^1\Sigma^+$ and $A^1\Sigma^+$ states.

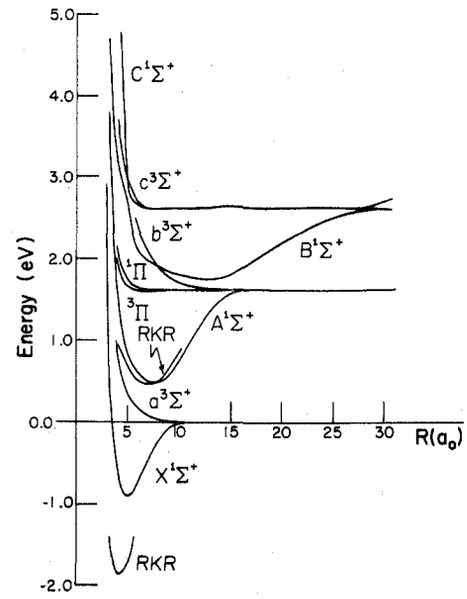

Figure 12. Same as Figure 11 except for KH.

It should be noted that the $C^1\Sigma^+$ states calculated here have no real physical significance since the ionic curve in the nonorthogonal basis will have another avoided crossing with the next higher covalent state of the same symmetry above the highest one considered here. The main reason for considering four $^1\Sigma^+$ states is that the addition of the fourth $^1\Sigma^+$ molecular basis function produces a fundamental difference in the calculated $B^1\Sigma^+$ state. In a three-state calculation omitting the $4^1\Sigma^+$ nonorthogonal diabatic state, the $B^1\Sigma^+$ state dissociates to the ionic configuration while in the four-state calculation it dissociates correctly to the M(n*s) + H(1s) atomic state. At values of R less than the position of the avoided crossing, the $B^1\Sigma^+$ in the three-state calculation has very little character of a molecular bound state. In the four-state calculation, however, a large amount of binding energy is added and the state resembles

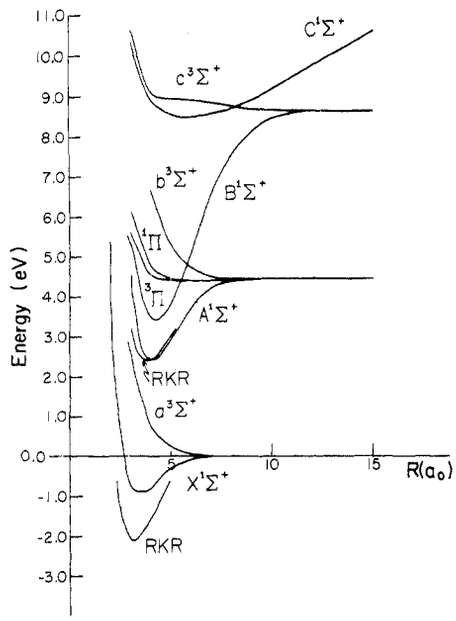

Figure 13. Same as Figure 11 except for MgH^+.

TABLE IV: Squares $|U_{ij}|^2$ of the Coefficients for the Expansion of the Adiabatic $^1\Sigma^+$ Wave Function in Terms of the Orthogonal Diabatic Basis Functions Near the Equilibrium Internuclear Distances of the Ground States

		Diabatic			
Adiabatic		Ionic	ns	np	$(n+1)$s
NaH	$X^1\Sigma^+$	0.487	0.426	0.066	0.021
$R = 4.0\ a_0$	$A^1\Sigma^+$	0.259	0.549	0.157	0.035
	$B^1\Sigma^+$	0.188	0.020	0.777	0.014
	$C^1\Sigma^+$	0.066	0.004	0.000	0.930
KH	$X^1\Sigma^+$	0.523	0.375	0.089	0.013
$R = 5.0\ a_0$	$A^1\Sigma^+$	0.089	0.474	0.429	0.008
	$B^1\Sigma^+$	0.029	0.032	0.151	0.788
	$C^1\Sigma^+$	0.359	0.120	0.331	0.191
MgH^+	$X^1\Sigma^+$	0.098	0.811	0.091	0.000
$R = 3.5\ a_0$	$A^1\Sigma^+$	0.770	0.120	0.010	0.100
	$B^1\Sigma^+$	0.031	0.064	0.896	0.008
	$C^1\Sigma^+$	0.101	0.005	0.003	0.891

the $A^1\Sigma^+$ state below it. Thus, the addition of the fourth molecular basis state to the calculation has given physical meaning to the $B^1\Sigma^+$ states.

At this point, it is interesting to examine the nature of the bonding $^1\Sigma^+$ molecular states. In Table IV we give the squares of the coefficients for the expansion of the adiabatic wave functions in terms of the symmetrically orthogonalized diabatic basis functions near $R = R_e$ for the ground state of the three molecules. Since symmetric orthogonalization has been used, these basis functions resemble the original nonorthogonal basis functions and we have labeled them as ionic, ns, np, and n*s according to the configurations to which they correspond in the limit of infinite separation.

Consider first the behavior of the eigenfunctions at large R. The $X^1\Sigma$ state changes character from covalent to ionic near $R = 7\ a_0$ for NaH and near $R = 8\ a_0$ for KH. The $A^1\Sigma^+$ state changes from covalent to ionic near $R = 12\ a_0$ for NaH and near $R = 15\ a_0$ for KH. The $B^1\Sigma^+$ state changes from covalent to ionic near $R = 23\ a_0$ for NaH and $R = 28\ a_0$ for KH. The $C^1\Sigma^+$ states change from ionic to covalent at the same places that the $B^1\Sigma^+$ states change from covalent to ionic but the covalent state comes in with a negative sign.

The ground state of MgH^+ is somewhat different from those of NaH and KH. This difference is due to the higher ionization potential of Mg^+ which prevents the ionic curve from descending low enough to interact in the same way with the lowest covalent state. There is, however, a change in character in the state at values of R less than $R = R_e$. The excited states exhibit characteristics similar to those of NaH and KH. The $A^1\Sigma^+$ state changes from covalent to ionic near $R = 6\ a_0$, the $B^1\Sigma^+$ state changes from covalent to ionic near $R = 10\ a_0$, and the $C^1\Sigma^+$ state changes from ionic to covalent at the same point with the covalent state coming in with a negative sign as it did in NaH and KH.

A very interesting result of these calculations is the fact that the triplet states also exhibit changes of character due to avoided crossings even though there is no simple physical explanation in terms of interactions with an ionic state since there is no ionic configuration in this case. The behavior of the triplet states for NaH and MgH^+ are qualitatively the same while KH is quite different. In fact, the $b^3\Sigma^+$ and $c^3\Sigma^+$ states for KH approach the behavior of a step function model. The change in character in these states takes place near $R = 5.5\ a_0$ over an interval of less than $0.1\ a_0$, and we shall find in the next section that the coupling matrices in this region are quite large and very narrow.

Near the equilibrium position, we see that the $X^1\Sigma^+$ states of NaH and KH are a mixture of the ionic and ns covalent states with the large component ionic as expected. The $X^1\Sigma^+$ state of MgH^+, however, is almost entirely covalent as we might have expected since we have seen that no curve crossing between the ionic and ns covalent states occurs in this case.

The $A^1\Sigma^+$ state for NaH is a mixture of the ionic state and the ns and np covalent states and is predominantly covalent. For KH the $A^1\Sigma^+$ state has a similar mixture of ionic and covalent states but has much less ionic character. The $A^1\Sigma^+$ state of MgH^+ is predominantly ionic.

The $B^1\Sigma^+$ states of NaH and MgH^+ are similar to each other having the character of the np configuration, while the same state for KH is dominated by the n*s state with a small component of np.

The nature of these states may be compared to the results of Melius et al.[36] for the excited states of LiH. They found that the $A^1\Sigma^+$ state has significant sp-hybrid character while the $B^1\Sigma^+$ state is essentially s-like in character. From the discussion above we see that our results for KH are in agreement with this picture of the molecular bonding but the results for NaH and MgH^+ are not in agreement. In other words, there appears to be more hybridization in LiH and KH than in NaH and MgH^+. In the former two cases the ionic configuration and the bonding sp-hybrid covalent configuration lead to the lowest two adiabatic potential curves and the n*s covalent configuration is lower in energy than the antibonding sp-hybrid covalent configuration. Although this effect is less important for NaH and MgH^+, we have performed additional calculations using only three molecular basis functions for NaH which show that the $B^1\Sigma^+$ adiabatic potential energy curve is still appreciably

TABLE V: Calculated and Experimental Equilibrium Distances R_e (in a_0) and Dissociation Energies D_e (in eV)

	$X^1\Sigma^+$				$A^1\Sigma^+$			
	R_e (expt)	R_e (calcd)	D_e'' (expt)	D_e'' (calcd)	R_e (expt)	R_e (calcd)	D_e' (expt)	D_e' (calcd)
NaH	3.572	4.121	2.05	1.085	6.064	6.115	1.33	1.303
KH	4.055	4.882	1.87	0.995	6.959	7.505	1.12	1.142
MgH^+	3.116	3.439	2.1	0.989	3.792	4.175	2.0	2.111

lowered near $R = R_e$ by addition of the fourth molecular basis function for NaH.

For small values of R, many changes occur in the character of the $^1\Sigma^+$ states for all three molecules. These changes are due to the presence of avoided crossings at small R and give rise to large coupling matrices in these regions as we shall see below. However, these avoided crossings may only be artifacts of the model used here and it is not clear whether they have any physical significance.

In Table V we present a comparison of experimental and calculated dissociation energies and equilibrium positions for the $X^1\Sigma^+$ and $A^1\Sigma^+$ states of the three molecules. The sources of the experimental values are explained in ref 30. From that table we see that we have been able to obtain almost all of the dissociation energy D_e' for the $A^1\Sigma^+$ states by the adjustment of the polarization potential but that the equilibrium position is shifted to larger R in each case. For the $X^1\Sigma^+$ states, about 53% of the dissociation energy has been obtained for NaH, 54% for KH, and 43% for MgH^+. The equilibrium positions for the $X^1\Sigma^+$ states are again too large.

It is interesting for comparison with Table V to note that Cade and Huo[37] made an extended basis Hartree–Fock calculation for the $X^1\Sigma^+$ state of NaH and obtained $D_e'' = 0.936$ eV and $R_e = 3.616\ a_0$. Szasz and McGinn[38] using the same model Hamiltonian as used in this work with their Phillips–Kleinman effective potential have reported values for R_e and D_e for the $X^1\Sigma^+$ states of NaH and KH. Using a trial wave function which is a linear combination of a covalent wave function and an ionic wave function both with adjustable parameters, they determined variationally the values $R_e = 3.77\ a_0$ and $D_e'' = 1.21$ eV for NaH and $R_e = 4.235\ a_0$ and $D_e'' = 0.916$ eV for KH. Adding a correlation factor to their wave function, they found $R_e = 3.78\ a_0$ and $D_e'' = 1.463$ eV for NaH and $R_e = 4.21\ a_0$ and $D_e'' = 1.230$ eV for KH.

In a valence bond calculation using a fixed minimum basis set of atomic orbitals which are optimized for the atoms and using complete configuration mixing, Heil, O'Neil, and Schaeffer[39] have found for the Cl_2 molecule that they obtain an equilibrium separation which is 18% larger than the experimental value and a dissociation energy which is only 29% of the experimental value. They attribute their poor results to the lack of flexibility within the molecular environment of the atomic orbitals in the valence bond model. The same effect has been pointed out previously by Harris and Michels[40] for the F_2 molecule.

In the work presented here, we have also used a valence bond model with a small (although larger than minimum basis set) set of fixed atomic orbitals which are optimized for the atoms but we have allowed only partial configuration mixing. It is clear that when only a few fixed atomic orbitals are included in the basis set and these orbitals are optimized for the atomic states rather than at small R, there will be a systematic error yielding relatively more accurate, i.e., lower, energies at larger R than at small R. This effectively shifts the calculated value of R_e toward larger R. We conclude that the poor values for R_e and D_e obtained here are due in large part to the inflexibility of our atomic orbitals, to the fact that they are optimized at large R, and to the fact that our orbital basis is not large enough rather than to a lack of other configurations which could be found using our orbital basis.

In Figure 14, we compare the ground state potential curve for NaH obtained by Cade and Huo[37] with the adiabatic states calculated here and with a set of adiabatic states calculated by Lewis, McNamara, and Michels.[41] The latter authors have performed a configuration mixing calculation in which only the valence electrons are promoted in excited configurations, i.e., they used the frozen core approximation. This approximation is similar physically to the effective potential formalism used in the present work but their choice of configurations differs from that used in the present work. The calculations of Lewis et al. are limited to $R > 4\ a_0$. From the figure we see that Lewis, McNamara, and Michels have obtained a larger and more accurate binding energy for the ground state than we have but that the binding energy we have obtained is larger than that obtained by Cade and Huo. The $A^1\Sigma^+$ potential curve obtained by Lewis, McNamara, and Michels has a completely incorrect shape compared to the RKR curve. Their II states, however, are probably better than the ones calculated here since we have included no configuration mixing for these states. Nevertheless, we see from Figure 14 that the II state curves obtained here have essentially the same shape as those obtained by Lewis, McNamara, and Michels and that their curves are lower in energy by only a few tenths of an electron volt. Part of the difference in the two $b^3\Sigma^+$ states is due to the presence of an avoided crossing in our calculation between the two highest $^3\Sigma^+$ states. This feature does not appear in the adiabatic potential curves of Lewis, McNamara, and Michels.

Comparison with other Work and Examination of the Curve Crossings. In the Introduction we indicated that the separation $\Delta W(R_c)$ between the adiabatic potential curves at the position $R = R_c$ of a crossing of two diabatic curves is important in the LZS model. Under the assumption that the system is described by a linear combination of two diabatic wave functions i and j, this separation is given by

$$\Delta W(R_c) = 2\left|H_{ij} - H_{ii}S_{ij}\right|/(1 - S_{ij}^2) \qquad (45)$$

where all quantities are to be evaluated at $R = R_c$. In eq 45 H_{ii} is the value of the two diagonal Hamiltonian matrix elements which cross at $R = R_c$ in the diabatic basis and H_{ij} is the matrix element between the two states which cross each other. The overlap between the two states is S_{ij}. In the nonorthogonal diabatic basis, eq 45 becomes

$$\Delta W(R_c^n) = 2\left|H_{ij}^n - H_{ii}^n S_{ij}\right|/(1 - S_{ij}^2) \qquad (46)$$

where the superscript n on R_c refers to the value of R_c in the nonorthogonal diabatic basis. In the symmetrically orthogonalized basis, eq 45 reduces to

$$\Delta W(R_c^s) = \left|2H_{ij}^s\right| \qquad (47)$$

where H_{ij}^s is the matrix element between the two states in the symmetrically orthogonalized basis evaluated at the

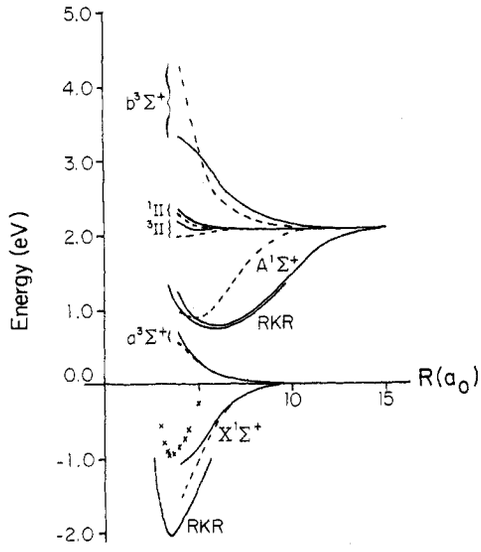

Figure 14. The adiabatic potential curves for NaH. The six dashed curves were calculated by Lewis, McNamara, and Michels and in each case the corresponding curve as calculated in the present work is shown for comparison. The X's are the results of Cade and Huo for the $X^1\Sigma^+$ state and the RKR curves are for the $X^1\Sigma^+$ and $A^1\Sigma^+$ states.

position R_c^s of the crossing of the symmetrically orthogonalized diabatic potential curves. As mentioned previously, R_c^s is not equal to R_c^n.

Using eq 46, the quantity ΔW has been calculated for the large R crossings for NaH and KH by Bates and Boyd[3] and the work has recently been repeated in modified fashion by Grice and Herschbach[4] for the crossing with the lowest covalent state for the same two molecules. The quantity ΔW has also been obtained for many other systems and the results have been tabulated by Olson, Smith, and Bauer.[42] It should be noted, however, that the values for H_{ij} listed in that tabulation are just half the values of ΔW given by Bates and Boyd. Thus Olson et al. assumed that Bates and Boyd were using an orthogonal representation which in fact they were not using.

Using the assumed $V_p(R)$ and the analytic forms which we have fit to our Hamiltonian matrix $\mathbf{H}^n(R)$ and to the transformation $\mathbf{C}(R)$, we have calculated the quantity ΔW from eq 46 for the nonorthogonal basis at the same values of R as were used by Bates and Boyd and by Grice and Herschbach. No crossings actually occur at these points in our model, but the calculations were performed to compare treatments. Since $H_{ii}^n(R_c) \neq H_{jj}^n(R_c)$ in our model, eq 46 is not really applicable to the present calculations at these R values; it is applied correctly at the positions of the crossings of the present model below. However, to compare our results to those of previous workers for the ionic–covalent curve crossings, we set H_{ii}^n in eq 46 equal to the asymptotic energy of the appropriate nonorthogonal diabatic covalent potential curve as they did. This is called procedure B in Table VI and the comparison of the results of procedure B with previous estimates of ΔW is essentially a comparison of calculated values of H_{ij}^n and S_{ij} for $i \neq j$. In addition, to illustrate the sensitivity of eq 46 to this choice we also used the equation with H_{ii}^n equal to the appropriate nonorthogonal diabatic covalent potential curve of the present work evaluated at $R = R_c$. These results are labeled procedure A in Table VI. Comparison of procedure A with procedure B shows that the results differ by 0.3–10%. Next we compare procedure B to the results of previous workers.

We give also in Table VI the three quantities P_1, P_2, P_3 which are defined as follows. P_1 is

$$P_1 = \Delta W_1/\Delta W_2 \tag{48}$$

where ΔW_1 is the value of ΔW calculated in the nonorthogonal representation in this work by procedure B and ΔW_2 is the value due to either Bates and Boyd or Grice and Herschbach. P_2 is

$$P_2 = \phi_1/\phi_2 \tag{49}$$

where ϕ_1 is the value of the pseudowave function used in this work evaluated at $x = R_c$ and ϕ_2 is the value of the coulomb approximation function used by Bates and Boyd. P_3 is

$$P_3 = \rho_1/\rho_2 \tag{50}$$

where ρ_1 is the probability density of finding an electron the distance $x = R_c$ from the proton as calculated from Goddard's GF function used in this work and ρ_2 is the same quantity calculated from either the Löwdin function used by Bates and Boyd or from the function used by Grice and Herschbach.

Considering first the crossings for the states dissociating to Na(3s) and K(4s), we see that the value for ΔW obtained here in the nonorthogonal basis is in good agreement with the value obtained by Bates and Boyd while the value given by Grice and Herschbach is much larger than the other two. These last authors attribute the difference between their results and those of Bates and Boyd to the difference in the H^- functions used. Detailed comparison of functions used for H^-, however, shows that the value of the probability density ρ corresponding to their H^- function is comparable to the ρ corresponding to the Löwdin function used by Bates and Boyd and actually smaller than the ρ for the GF function used here in the region from 7 to 9 a_0. On this basis alone, one would expect Grice and Herschbach to obtain a smaller value of ΔW. It is interesting to note that Grice and Herschbach used Whittaker functions for the alkali wave functions. The only difference for large x between these functions and the coulomb approximation functions used by Bates and Boyd is the normalization constant which appears in the equation used by Bates and Boyd but not in the equation used by Grice and Herschbach. Comparison with a numerical Hartree–Fock wave function for K (see above) shows that this constant leads to radial wave functions which are accurately normalized in the asymptotic region for the ground s state and it is interesting to note that for Na(3s) it has the value 0.543 and for K(4s) it has the value 0.537. Multiplying the values of ΔW due to Grice and Herschbach by these values we find $\Delta W = 1.54 \times 0.543 = 0.836$ eV for Na(3s) and $\Delta W = 1.06 \times 0.537 = 0.569$ eV for K(4s). These results are in much better agreement with the present results and the results obtained by Bates and Boyd. Therefore, it seems as though a great deal of the difference in the results is due to the lack of normalization of the alkali functions used by Grice and Herschbach.

We see from the table that we obtain better agreement, in general, with previous work when we evaluate H_{ii}^n at the asymptotic energies since this was the assumption made in the previous studies. Our results on the whole agree fairly well with those of Bates and Boyd but the differences seem to have no correlation with the differences in the wave

TABLE VI: Comparison of the Energy Separation $\Delta W(R_c)$ in Electron Volts with Previously Calculated Values at the Positions R_c (in bohrs) of Previously Determined Avoided Crossings

State[a]	R_c	ΔW			P_1[d]	P_2[e]	P_3[f]	P_2P_3
		Previous work	This work A[b]	This work B[c]				
Na(3s)	7.7	0.585 (BB)[g]	0.520	0.573	0.98	0.99	3.2	3.1
Na(3s)	7.55	1.54 (GH)	0.564	0.627	0.41		3.3	
Na(3p)	12.6	0.320 (BB)	0.278	0.286	0.89	0.38	9.7	0.37
Na(4s)	22.9	4.35×10^{-2} (BB)	7.90×10^{-2}	7.88×10^{-2}	1.81	0.39	79.0	31.0
K(4s)	8.8	0.495 (BB)	0.455	0.492	0.99	0.83	4.0	3.3
K(4s)	8.8	1.06 (GH)	0.455	0.492	0.46		3.5	
K(4p)	14.3	0.242 (BB)	0.235	0.233	0.96	0.32	12.0	3.8
K(5s)	27.7	1.90×10^{-2} (BB)	3.18×10^{-2}	3.19×10^{-2}	1.68	0.35	23.0	8.1

[a] The state which crosses the ionic state at $R = R_c$. [b] Obtained with H_{ii}^n equal to the appropriate nonorthogonal diabatic covalent matrix element. [c] Obtained with H_{ii}^n equal to the asymptote of the covalent state. [d] Equation 48. [e] Equation 49. [f] Equation 50. [g] BB denotes Bates and Boyd; GH denotes Grice and Herschbach.

functions used. One might naively expect, since the crossings occur at large R, that the difference in ΔW would have contributions from the differences in the atomic wave functions of the electron transferred in a given transition between two diabatic states so that $P_1 \simeq P_2P_3$. However, the values given in the table show that this is not even approximately true.

As mentioned above, no actual curve crossings occur in our model at the positions listed in Table VI. Again using the analytic forms for the matrices $\mathbf{H}^n(R)$ and $\mathbf{C}(R)$ and the polarization potential $V_p(R)$ we have determined all of the curve crossings which occur for all three molecules in both the nonorthogonal diabatic and the orthogonal diabatic representations. The positions R_c of these crossings are given in Tables VII–IX. We notice first of all that the total number of crossings is not constant from one representation to the other. Especially interesting is the fact that no crossing occurs between the $1^1\Sigma^+$ and $2^1\Sigma^+$ states for NaH in the nonorthogonal basis but two crossings occur in the orthogonal basis. It is also interesting that for all three molecules the orthogonalization process introduces new crossings at small values of R between the ionic and covalent states as well as crossings between the covalent states. For those crossings which occur in both representations the position of the crossing is not constant. Some of these positions may shift as much as 1 a_0 or even 2 a_0 for small values of R_c while the ones occurring at larger values of R_c tend to shift by only a few tenths of 1 a_0.

We shall see below that, although the results in the adiabatic representation are independent of the method of orthogonalization, the curve crossings which occur in the symmetrically orthogonalized diabatic basis are of fundamental importance in determining the character of the coupling matrices between adiabatic electronic states. The large R crossing points for $^1\Sigma^+$ states have an obvious physical interpretation in terms of interactions between the ionic and covalent configurations. The small R crossings for the $^1\Sigma^+$ states and all the crossings for $^3\Sigma^+$ states have no such obvious interpretation and may just be artifacts of the original nonorthogonal basis chosen or of the model Hamiltonian assumed. Further work with larger basis sets is required to better understand the $^1\Sigma^+$ and $^3\Sigma^+$ manifolds at small R.

Since the LZS model places a great deal of importance on the quantity ΔW at the points $R = R_c$, we have calculated these quantities from our analytic forms for all crossings given in the tables and the values obtained are listed in Tables VII–IX. For the nonorthogonal diabatic representation we have used eq 46 and for the symmetrically orthogonalized diabatic basis we have used eq 47.

It will be recalled that the quantity ΔW given by eq 46 for a nonorthogonal basis and eq 47 for an orthogonal basis is the energetic separation between the two adiabatic potential curves at the position of an avoided crossing under the assumption that the system is described in terms of a two-state basis. Here we are dealing with a four-state system ($^1\Sigma^+$ manifold) and a three-state system ($^3\Sigma^+$ manifold) and it is not true that the values of ΔW obtained from eq 46 or 47 will be equal to the actual separation between the adiabatic potential curves. We have therefore determined the actual separation $\Delta W'$ between these curves at the positions of the avoided crossings using the curves obtained from our analytic forms. These values are also listed in the tables for comparison with ΔW.

If a particular avoided crossing is adequately described in terms of two of the present diabatic states, then ΔW and $\Delta W'$ will be approximately equal. From the results in Tables VII–IX we see that in general for the large R crossings the two quantities are approximately equal while for small R crossings some of the values are about equal but the majority are not. Thus, it would seem that the large R crossings may indeed be treated in terms of a two-state model in the present diabatic basis but the small R crossing in general may not.

The Coupling Matrices in the Adiabatic Representation. Next we present results for the matrices **M** and **N** and analyze their characteristics in terms of the relative contributions of the matrices $\mathbf{M}_1$, $\mathbf{M}_2$, $\mathbf{N}_1$, and $\mathbf{N}_2$.

The properties of **M** and **N** are determined by the derivatives of the matrix elements of the two matrices **C** and **U** according to eq 37–44. We recall that the matrix **C** is the transformation from the nonorthogonal to the orthogonal diabatic basis and that the matrix elements of **C** are fairly slowly varying functions of R. Therefore, we expect to find that the matrix elements of $\mathbf{M}_1$ and $\mathbf{N}_1$ are fairly small. The matrix **U** is the transformation which diagonalizes the electronic Hamiltonian in the orthogonal diabatic basis and the matrix elements of **U** as functions of R change very rapidly in certain regions corresponding to the change in character of the adiabatic states in the regions of avoided crossings. We expect therefore that the elements of $\mathbf{M}_2$ and $\mathbf{N}_2$ will be somewhat larger than those of $\mathbf{M}_1$ and $\mathbf{N}_1$ and that the elements of $\mathbf{M}_2$ will have peaks in the regions where the avoided crossings occur in the symmetrically orthogonalized di-

TABLE VII: Curve Crossing Positions R_c (in bohrs) for NaH States for Both the Nonorthogonal and Orthogonal Diabatic Bases and the Separation (in eV) between Adiabatic Potentials at R_c where ΔW is from Eq 46 or 47 and $\Delta W'$ is Measured from the Calculated Curves

	$i = 2$			$i = 3$			$i = 4$		
j	R_c	ΔW	$\Delta W'$	R_c	ΔW	$\Delta W'$	R_c	ΔW	$\Delta W'$
$^1\Sigma^+$ nonorthogonal									
1				12.45	0.296	0.319	23.02	7.81×10^{-2}	7.93×10^{-2}
$^1\Sigma^+$ orthogonal									
1	4.28	2.10	2.14	3.22	1.84	1.62	2.83	0.132	2.53
1	4.86	1.86	1.82	12.32	0.332	0.329	23.09	7.88×10^{-2}	7.89×10^{-2}
2				2.49	0.314	3.46	2.13	5.34	1.56
$^3\Sigma^+$ nonorthogonal									
1	1.83	4.18	1.72	1.67	2.72	4.44			
$^3\Sigma^+$ orthogonal									
1	1.86	4.34	1.75	1.77	2.70	3.81			
2				2.59	0.954	1.68			
2				4.82	6.44×10^{-2}	0.220			

TABLE VIII: Curve Crossing Positions R_c (in bohrs) for KH States for Both the Nonorthogonal and Orthogonal Diabatic Bases and the Separation (in eV) between Adiabatic Potentials at R_c where ΔW is from Eq 46 or 47 and $\Delta W'$ is Measured from the Calculated Curves

	$i = 2$			$i = 3$			$i = 4$		
j	R_c	ΔW	$\Delta W'$	R_c	ΔW	$\Delta W'$	R_c	ΔW	$\Delta W'$
$^1\Sigma^+$ nonorthogonal									
1	4.33	2.12	2.09	2.31	1.75	1.69	1.57	2.31	27.3
1	6.77	1.08	1.04	14.31	0.234	0.239	28.00	3.12×10^{-2}	3.19×10^{-2}
$^1\Sigma^+$ orthogonal									
1	5.68	1.88	1.55	4.43	3.12	1.64	4.12	0.254	2.82
1	6.67	1.25	1.08	14.50	0.228	0.225	28.16	3.12×10^{-2}	3.12×10^{-2}
2				3.79	1.64	2.17	3.49	1.60	1.59
$^3\Sigma^+$ nonorthogonal									
1	1.96	3.92	1.28	1.84	2.49	4.40			
$^3\Sigma^+$ orthogonal									
1	1.98	4.06	1.30	1.93	2.52	3.94			
2				3.67	0.506	0.786			
2				4.71	0.198	0.343			

TABLE IX: Curve Crossing Positrons R_c (in bohrs) for MgH^+ States for Both the Nonorthogonal and Orthogonal Diabatic Bases and the Separation (in eV) between Adiabatic Potentials at R_c where ΔW is from Eq 46 or 47 and $\Delta W'$ is Measured from the Calculated Curves

	$i = 2$			$i = 3$			$i = 4$		
j	R_c	ΔW	$\Delta W'$	R_c	ΔW	$\Delta W'$	R_c	ΔW	$\Delta W'$
$^1\Sigma^+$ nonorthogonal									
1				4.10	2.18	1.09	9.99	0.521	0.635
1				5.53	1.60	1.22			
$^1\Sigma^+$ orthogonal									
1				3.56	1.02	0.667	2.20	1.90	2.97
1				5.89	1.42	1.31	9.73	0.626	0.642
$^3\Sigma^+$ nonorthogonal									
1	1.73	18.6	5.71	1.59	4.37	21.7			
$^3\Sigma^+$ orthogonal									
1	1.74	20.4	15.6	1.94	2.08	6.27			
2				2.64	0.374	2.15			

abatic basis while the elements of N_2 will go through a change in sign at these points.

The results of the calculations of the coupling matrices **M** and **N** are shown in Figures 15–22 and A3–A6[34] where we have plotted the matrix elements as functions of internuclear distance. We have plotted the elements of the ma-

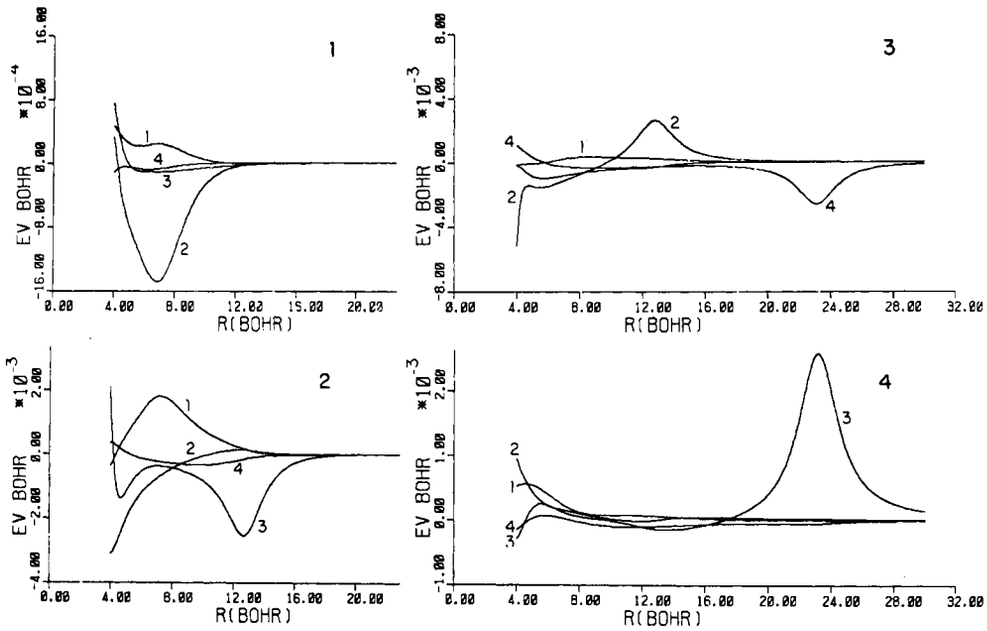

Figure 15. The coupling matrix elements M_{ij} for the $^1\Sigma^+$ states of NaH as functions of internuclear distance R. Each of the four subfigures corresponds to one column j and each curve is labeled by the row index i.

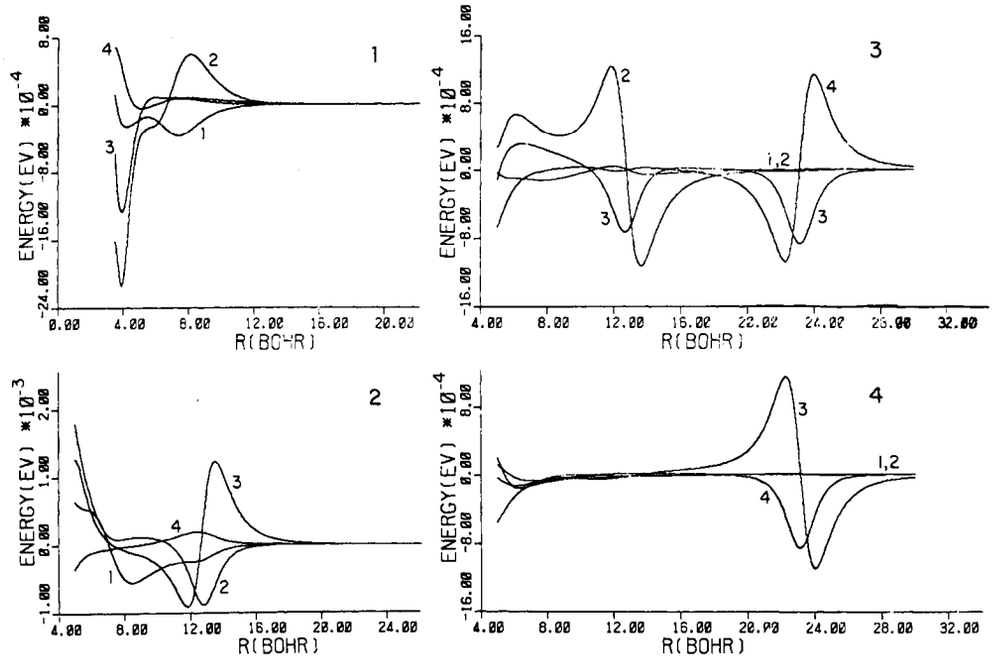

Figure 16. Same as Figure 15 except the coupling matrix elements N_{ij} for the $^1\Sigma^+$ states of NaH are shown.

trices column by column and the number of each curve refers to the component of the column being plotted for that particular curve.

Recalling the ordering convention for the adiabatic states, i.e., lowest energy first at each value of R (see above), we see for example that curve 2 of column 1 is the interaction between the $X^1\Sigma^+$ state and the $A^1\Sigma^+$ state, curve 3 of column 1 is the interaction between $X^1\Sigma^+$ state and the $B^1\Sigma^+$ state, curve 4 of column 1 is the interaction between the $X^1\Sigma^+$ state and the $C^1\Sigma^+$ state, etc.

For the $^1\Sigma^+$ states, it was necessary to make two graphs for each matrix: one for large values of R, in general greater than about 4 a_0, and one for small values of R. The results for large R are shown in Figures 15–18 and A3 and A4;[34] the results at small R are given in ref 30. For the $^3\Sigma^+$ states the results are shown in Figures 19–22 and A5 and A6.[34]

Comparing the matrix $\mathbf{M}$ with the matrix $\mathbf{M}_2$ shows that qualitatively the major contributor to the matrix $\mathbf{M}$ is the matrix $\mathbf{M}_2$ and that the matrix $\mathbf{M}_1$ adds only a small amount. However the contributions from $\mathbf{M}_1$ are important.

The elements of the matrix $\mathbf{N}_1$ are in general quite small at large values of R and have significant size only at small R where the matrix $\mathbf{C}(R)$ has large derivatives. The product matrix $4\mu\mathbf{M}_1\mathbf{M}_2$ is also small and therefore the main contribution to the matrix $\mathbf{N}$ comes from the matrix $\mathbf{N}_2$.

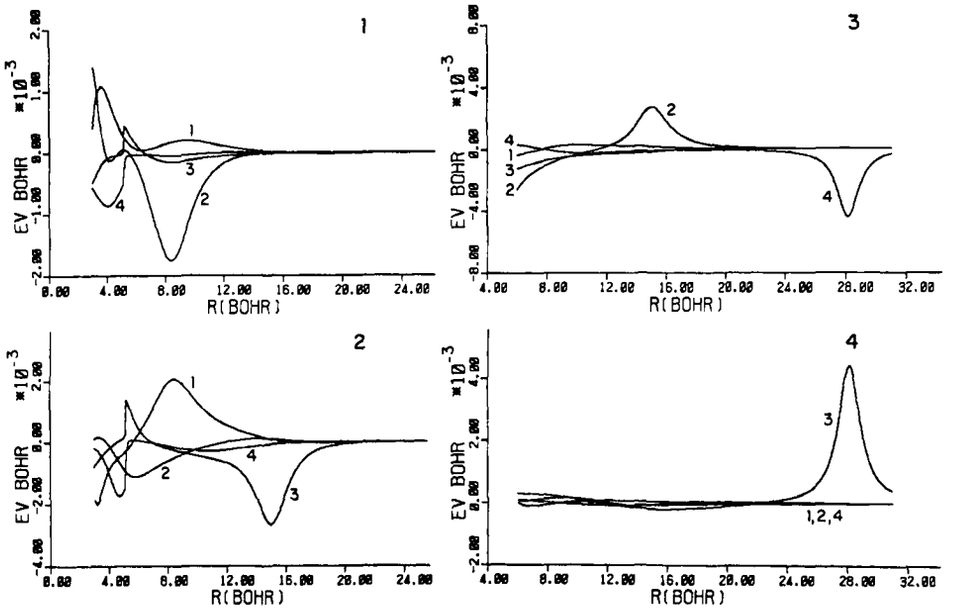

Figure 17. Same as Figure 15 except the coupling matrix elements M_{ij} for the $^1\Sigma^+$ states of KH are shown.

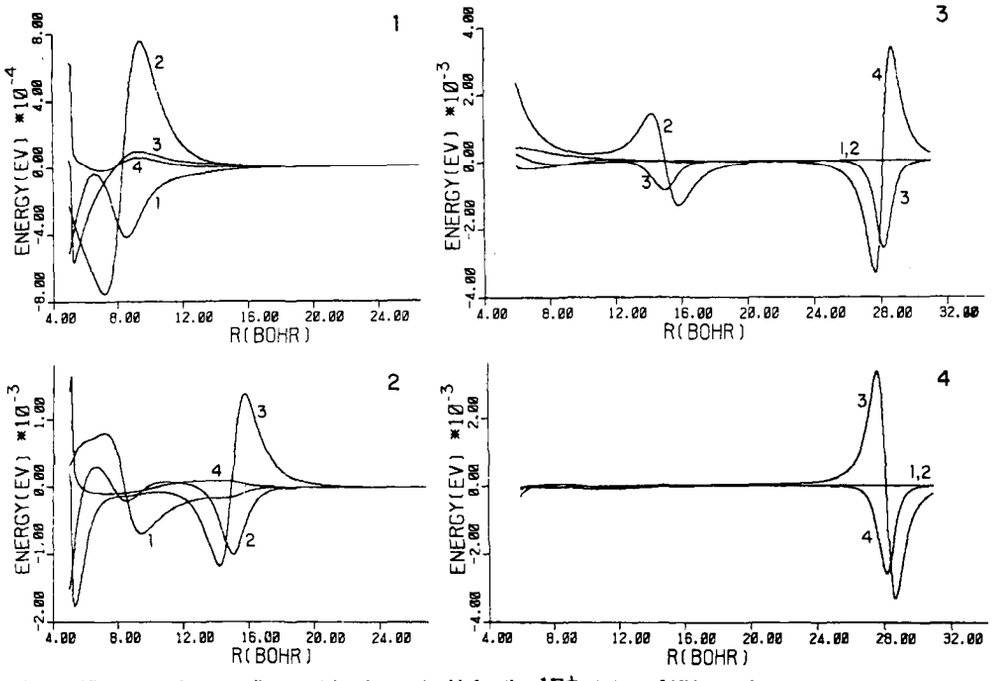

Figure 18. Same as Figure 15 except the coupling matrix elements N_{ij} for the $^1\Sigma^+$ states of KH are shown.

From eq 43 we see that $\mathbf{N}_2$ is related to the derivatives of the matrix **U** which diagonalizes the matrix $\mathbf{H}^s$ so that properties of both the matrix **M** and the matrix **N** are mainly related to the diagonalization of $\mathbf{H}^s$ rather than to the orthogonalization of the basis functions.

We discuss first the results for the $^1\Sigma^+$ states at large values of R. For the matrix **M** shown in Figure 15 for NaH, Figure 17 for KH, and Figure A3[34] for MgH^+, the most prominent feature is the existence of broad peaks in certain matrix elements. For NaH, the matrix elements M_{21} and M_{12} peak near 7 a_0 and the position of this peak correlates with the change in character of the $X^1\Sigma^+$ wave function which appears as a crossing of elements 1 and 2 of column 1 of the matrix **A**. The matrix elements M_{32} and M_{23} peak near 13 a_0 and this position correlates with the change in character of the $A^1\Sigma^+$ wave function which appears as a crossing of elements 1 and 3 of column 2 of the matrix **A**. The matrix elements M_{43} and M_{34} peak near 23 a_0 and this position correlates with the change in character of the $B^1\Sigma^+$ wave function which appears as a crossing of elements 1 and 4 of column 3 of the matrix **A**. Similar correlations may be made for KH and MgH^+. The same may be done for the triplet states for all three molecules.

The fact that the matrix elements of **M** which couple different adiabatic electronic states are large over a very wide range of R values raises serious questions concerning the Landau–Zener–Stueckelberg treatment of the curve crossing problem. This model assumes that transitions from one adiabatic curve to another take place only at the positions of avoided crossings and that coupling between these states

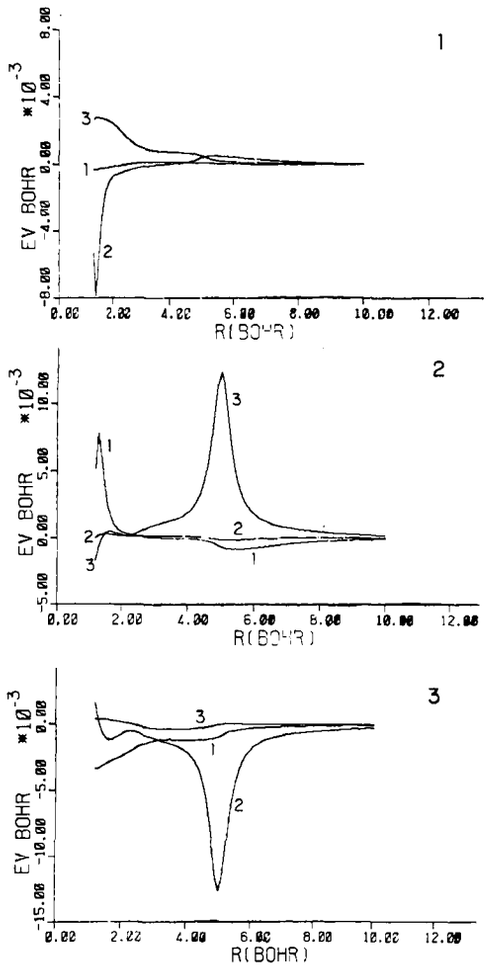

Figure 19. Same as Figure 15 except the coupling matrix elements M_{ij} for the $^3\Sigma^+$ states of NaH are shown.

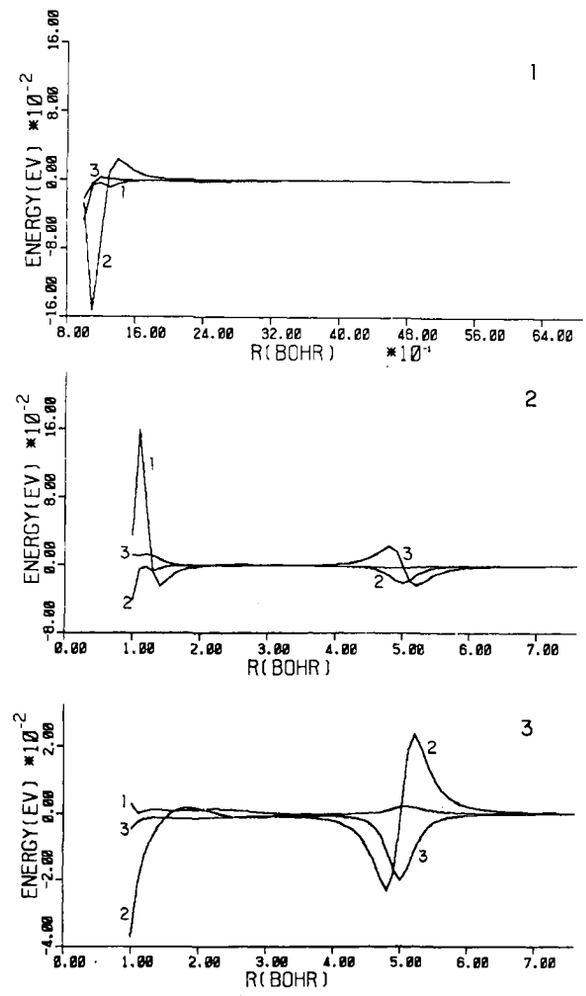

Figure 20. Same as Figure 15 except the coupling matrix elements N_{ij} for the $^3\Sigma^+$ states of NaH are shown.

at other values of R is negligible. From our results, however, we see that the coupling elements of the matrix **M** are significant over large regions as wide as 10–12 a_0 in some cases.

We may compare the sizes and shapes of our matrix elements for **M** to those calculated by Oppenheimer[43] in the London model[44] for KI for the avoided crossing between ionic and covalent configurations which occurs near $R = 21$ a_0 in that system. Oppenheimer obtains a very sharply peaked coupling matrix element near $R = 21$ a_0 over a region of width about 2 a_0. Dividing through by twice the reduced mass of the KI molecule to convert to the same units as presented here, we find that the peak has a maximum value of about 5.1×10^{-3} eV bohr. We compare this value to our coupling matrix element M_{34} for the avoided crossing near $R = 28$ a_0 for KH which is large over a region of width about 8 a_0 and has a maximum value of about 4.3×10^{-3} eV bohr. Thus the adiabatic states in KI change character over a much smaller range of R values than do those for KH while the size of the coupling matrix is about the same in the two cases.

We turn now to the results for the matrix **N** for the $^1\Sigma^+$ states shown for large values of R in Figure 16 for NaH, in Figure 18 for KH, and in Figure A4[34] for MgH^+. We note first of all that at the positions where the off-diagonal elements of the matrix **M** go through maxima as described above the corresponding elements of the matrix **N** go through zero. This relation might have been expected since the matrix **M** is given in terms of the first derivative of the matrix **A** as defined in eq 37 and the matrix **N** is given in terms of the second derivative of the matrix **A** as defined in eq 41.

Another feature of the results is the existence of peaks in the diagonal elements of **N** at the positions of zeroes of corresponding off-diagonal elements. For example, for the $^1\Sigma^+$ state of NaH shown in Figure 16 the elements N_{33} and N_{44} both have peaks at the zeroes of the elements N_{34} and N_{43}. In the adiabatic approximation described by Wolniewicz[45] and Hirschfelder and Meath[6] the diagonal elements of all coupling matrices are added to the potential energy curve $W_k(R)$. From eq 27, 40, and 44 we see that in the adiabatic representation the matrix G^a is given by

$$\mathbf{G}^a = \mathbf{A}^\dagger \mathbf{G}^n \mathbf{A} - i4\mu \mathbf{A}^\dagger \bar{\mathbf{F}}^n \mathbf{A} \cdot \mathbf{M} \hat{e}_R - \mathbf{N} \qquad (51)$$

From the figures, we see that the peaks in the diagonal elements of **N** are always negative and that therefore these matrix elements will make positive contributions to the adiabatic potential energy curves. These contributions are on the order of 10^{-3} eV for the $^1\Sigma^+$ states.

The coupling matrices for the $^3\Sigma^+$ states are shown for NaH in Figures 19 and 20, for KH in Figures 21 and 22, and for MgH^+ in Figures A5 and A6.[34] The matrix elements for

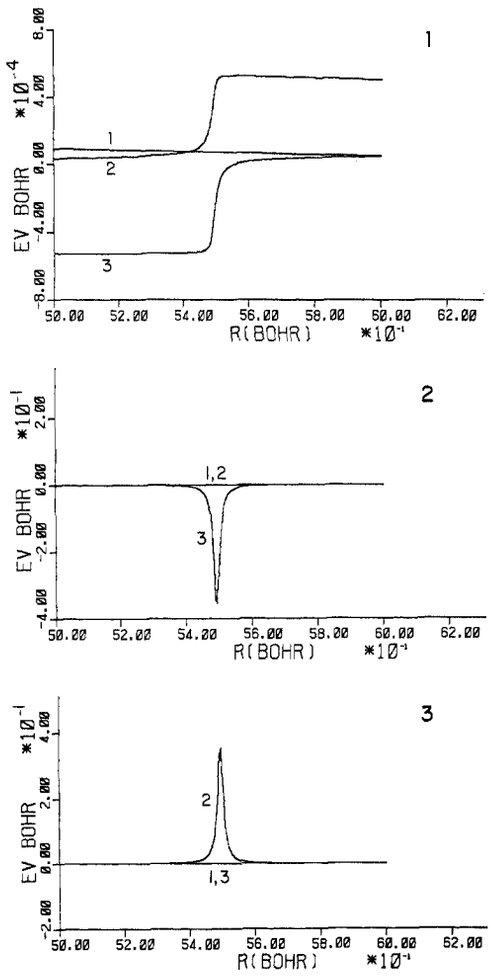

Figure 21. Same as Figure 15 except the coupling matrices M_{ij} for the $^3\Sigma^+$ states of KH are shown.

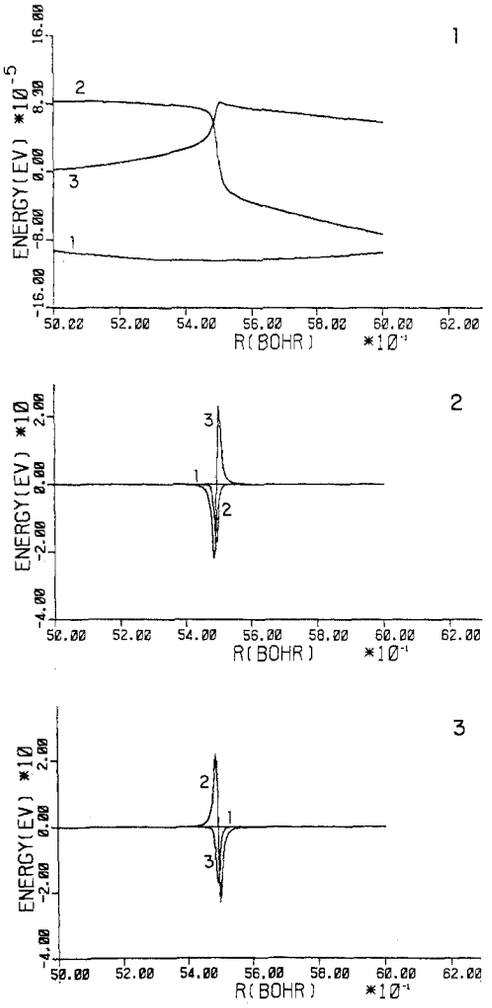

Figure 22. Same as Figure 15 except the coupling matrices N_{ij} for the $^3\Sigma^+$ states of KH are shown.

NaH and MgH^+ are quite similar while those for KH are somewhat different. The differences for KH are due to the rapid change in character of the $b^3\Sigma^+$ and $c^3\Sigma^+$ states in a very narrow region near $R = 5.5\ a_0$ which we have mentioned above. To show clearly the nature of the matrix elements for KH in this region we have restricted the range of R values included in Figures 21 and 22.

The most prominent feature of the coupling matrices for the $^3\Sigma^+$ states is the existence of peaks in the elements M_{12}, M_{21}, M_{23}, and M_{32} which in turn lead to corresponding variations in the elements of the matrix **N**. We note that the matrix elements M_{23} and M_{32} for NaH are of the same sign and about the same order of magnitude as the corresponding elements for MgH^+ and that they extend over a fairly wide range of R values, about 5 a_0 fo. NaH and about 2 a_0 for MgH^+. For KH, however, the corresponding elements are of opposite sign, are an order of magnitude larger, and are much narrower, extending over a range of only about 0.1 a_0. We have mentioned above that the change in character of the adiabatic states for KH in this region of R approaches the behavior of a step function and the corresponding coupling matrix elements approach the behavior of a delta function.

Note the very large matrix elements N_{23}, N_{32}, N_{22}, and N_{33} for the KH $^3\Sigma^+$ states shown in Figure 22 near $R = 5.5$ a_0. These matrix elements have magnitudes as large as 20 eV. As discussed above for the $^1\Sigma^+$ states, the diagonal elements N_{22} and N_{33} are included in the adiabatic effective internuclear potential energy curves in the adiabatic approximation of Wolniewicz and Hirschfelder and Meath. These potential curves would therefore have very narrow positive peaks of height 20 eV near $R = 5.5\ a_0$. This approximation gives an upper bound to the true electronic eigenvalues.[6] It is not clear in this case whether the upper bound thus obtained would be a good one.

Evans, Cohen, and Lane[46] have applied the London model[44] to the curve crossing problem for the excited triplet states of He_2, and although the crossing in that system is of a different type from the ones considered here, we may compare the coupling matrix elements obtained by those authors with the ones obtained here. Dividing the maximum value of their peak by twice the reduced mass of He_2, we find that their matrix element has a maximum value of about 2.0×10^{-3} eV bohr at $R = 3\ a_0$ with a width of about 2 a_0. This value may be compared with the M_{32} element for NaH which has a maximum of about 13×10^{-3} eV bohr near $R = 5\ a_0$ with a width of about 2 a_0.

At small values of R the matrix elements are much larger and vary more rapidly over very short intervals. However, an accurate treatment of the dynamics at small R may require more complete calculations than the present ones. As mentioned above, our original nonorthogonal valence bond basis set was chosen to describe the physics of the problem

at large values of R and the atomic orbitals are not allowed to adjust as the atoms approach each other. We know that our potential curves are not as accurate at small R as at large R and the behavior of the coupling matrices at small R may therefore be only an artifact of our model. However, the qualitative features of our results do indicate that an accurate treatment of the small R region would be interesting.

The effect of large coupling matrices at small values of R on the cross section obtained in a scattering calculation is not clear until the actual calculations are performed. At thermal energies they will probably not be important since they occur in the region beneath the high repulsive wall of adiabatic potential energy curves. Furthermore, they will contribute only to the lowest partial waves since the centrifugal barrier at higher angular momenta will prevent the atoms from approaching the region where the coupling is large. The coupling matrix elements at large R, however, will provide large contributions to the quenching since the cross section is approximately proportional to the square of the distance at which the transition occurs and thus because many more partial waves will contribute. Therefore, even though the coupling matrices at small R are much larger than those at large R, it is expected that they will not contribute as much to the quenching cross section.

We emphasize at this point that the results presented here are independent of the method of orthogonalization used. For example, suppose we orthogonalize the nonorthogonal diabatic basis by multiplication by the matrix $\mathbf{CX}$ where $\mathbf{X}$ is an arbitrary unitary matrix so that

$$\phi^{\circ} = \phi^{n}\mathbf{CX} \tag{52}$$

Equation 52 is consistent with our general form of orthogonalization as discussed above (see eq 22). The Hamiltonian matrix in this representation is given by

$$\mathbf{H}^{\circ} = \mathbf{X}^{\dagger}\mathbf{H}^{s}\mathbf{X} \tag{53}$$

and the adiabatic Hamiltonian matrix is given by

$$\mathbf{H}^{a} = (\mathbf{X}^{\dagger}\mathbf{U}^{\dagger})^{\dagger}\mathbf{H}^{\circ}\mathbf{X}^{\dagger}\mathbf{U} \tag{54}$$

where the unitary matrix $\mathbf{U}$ is defined by eq 24. Therefore, the unitary matrix which diagonalizes $\mathbf{H}^{\circ}$ is the product matrix $\mathbf{X}^{\dagger}\mathbf{U}$ and the matrix $\mathbf{A}^{\circ}$ which transforms from the nonorthogonal to the adiabatic representation is given by

$$\mathbf{A}^{\circ} = \mathbf{CXX}^{\dagger}\mathbf{U} = \mathbf{A} \tag{55}$$

Thus, the transformation $\mathbf{A}$ and hence also its derivatives are independent of the method of orthogonalization. Likewise for the matrix $\mathbf{M}^{\circ}$ in this representation, we have

$$\mathbf{M}^{\circ} = \frac{1}{2\mu}(\mathbf{X}^{\dagger}\mathbf{U})^{\dagger}(\mathbf{CX})^{-1}\,\mathrm{d}\mathbf{A}^{\circ}/\mathrm{d}R = \mathbf{M} \tag{56}$$

so that the matrix $\mathbf{M}$ and by a similar argument the matrix $\mathbf{N}$ are also independent of the method of orthogonalization.

As we have seen, the character of the elements of the matrix $\mathbf{A}$ as functions of R is chiefly determined by the character of the elements of the matrix $\mathbf{U}$. The character of these elements is in turn determined by the positions of the curve crossings of the diagonal elements of the symmetrically orthogonalized diabatic electronic Hamiltonian matrix $\mathbf{H}^{s}$. Therefore, since the matrix $\mathbf{A}$ is independent of the method of orthogonalization, the positions of the curve crossings in the symmetrically orthogonalized diabatic representation are of fundamental importance in determining the nature of the coupling between adiabatic states.

It will be noticed from the figures that the matrix $\mathbf{M}$ is not skew symmetric which may be seen from the fact that the diagonal elements are not zero and the peaks corresponding to transposed elements are shifted slightly with respect to each other and are of different absolute magnitude. However the matrix $\mathbf{M}_2$ is skew symmetric which follows from the fact that the matrix $\mathbf{U}$ is unitary. We have in fact

$$\mathrm{d}(\mathbf{U}^{\dagger}\mathbf{U})/\mathrm{d}R = 0 = (\mathrm{d}\mathbf{U}^{\dagger}/\mathrm{d}R)\mathbf{U} + \mathbf{U}^{\dagger}(\mathrm{d}\mathbf{U}/\mathrm{d}R) \tag{57}$$

so that

$$\mathbf{U}^{\dagger}(\mathrm{d}\mathbf{U}/\mathrm{d}R) = -(\mathrm{d}\mathbf{U}^{\dagger}/\mathrm{d}R)\mathbf{U} = -(\mathbf{U}^{\dagger}(\mathrm{d}\mathbf{U}/\mathrm{d}R))^{\dagger} \tag{58}$$

and therefore from eq 39 we have

$$\mathbf{M}_2 = -\mathbf{M}_2^{\dagger} \tag{59}$$

We recall from eq 26b and 40 that one of the coupling matrices in the adiabatic representation which appears in the coupled differential equations for the nuclear motion, eq 21, is given by

$$\vec{\mathbf{F}}^{a} = \mathbf{A}^{\dagger}\vec{\mathbf{F}}^{n}\mathbf{A} - i\mathbf{M}\hat{e}_R \tag{60}$$

Since the adiabatic representation is real and orthogonal for the Σ states, the matrix $\vec{\mathbf{F}}^{a}$ for the Σ states is skew symmetric. Therefore, since $\mathbf{M}_2$ is also skew symmetric, the diagonal elements of the matrix $\mathbf{M}_2$ must be equal to the negatives of the corresponding diagonal elements of the radial component of the matrix $\mathbf{A}^{\dagger}\vec{\mathbf{F}}^{n}\mathbf{A}$.

With these results, we see from eq 51 and 60 that the coupling matrices $\vec{\mathbf{F}}^{a}$ and $\mathbf{G}^{a}$ in the adiabatic representation are also independent of the method of orthogonalization although of course they do depend on the initial nonorthogonal basis assumed. We recall furthermore that we have not calculated the matrices $\vec{\mathbf{F}}^{n}$ and $\mathbf{G}^{n}$ so that we have only obtained a portion of the total coupling matrices, i.e., the part corresponding to the matrices $\mathbf{M}$ and $\mathbf{N}$. We have also noted that the matrix $\mathbf{M}$ is not skew symmetric while the matrix $\vec{\mathbf{F}}^{a}$ must be skew symmetric. One method of avoiding this problem is to note that the matrix $\vec{\mathbf{F}}^{a}$ may also be written

$$\vec{\mathbf{F}}^{a} = \mathbf{U}^{\dagger}\vec{\mathbf{F}}^{s}\mathbf{U} - i\mathbf{M}_2\hat{e}_R \tag{61}$$

We could neglect the first term of eq 61 instead of neglecting the first term of eq 60 and use the skew symmetric matrix $\mathbf{M}_2$ as an approximation for the coupling matrix $\vec{\mathbf{F}}^{a}$. However, the matrix $\mathbf{M}_2$ is not independent of the method of orthogonalization since for the orthogonalization according to eq 52 we have

$$\mathbf{M}_2^{\circ} = \frac{1}{2\mu}(\mathbf{X}^{\dagger}\mathbf{U})^{\dagger}\mathrm{d}(\mathbf{X}^{\dagger}\mathbf{U})/\mathrm{d}R \tag{62a}$$

$$= \mathbf{M}_2 + \frac{1}{2\mu}\mathbf{U}^{\dagger}\mathbf{X}(\mathrm{d}\mathbf{X}^{\dagger}/\mathrm{d}R)\mathbf{U} \tag{62b}$$

To avoid this difficulty we suggest the following procedure. We may write the identity

$$\mathbf{M} = \mathbf{M}_3 + \mathbf{M}_4 \tag{63}$$

where $\mathbf{M}_3$ is the skew symmetric matrix

$$\mathbf{M}_3 = \tfrac{1}{2}(\mathbf{M} - \mathbf{M}^{\dagger}) \tag{64}$$

and $\mathbf{M}_4$ is the symmetric matrix

$$\mathbf{M}_4 = \tfrac{1}{2}(\mathbf{M} + \mathbf{M}^\dagger) = \tfrac{1}{2}(\mathbf{M}_1 + \mathbf{M}_1^\dagger) \quad (65)$$

where the contribution of $\mathbf{M}_2$ to the matrix $\mathbf{M}_4$ is cancelled since $\mathbf{M}_2$ is skew symmetric. We may now neglect the matrix $\mathbf{M}_4$ which is small since the matrix elements of $\mathbf{M}_1$ are in general small. Then our approximation for the matrix $\vec{\mathbf{F}}^a$ would be the skew symmetric matrix $\mathbf{M}_3$ defined by eq 64 which is independent of the method of orthogonalization since the matrix $\mathbf{M}$ is.

Similarly, for the matrix $\mathbf{G}^a$, which must appear as a symmetric matrix in the coupled differential equations for the nuclear motion, we form the identity

$$\mathbf{N} = \mathbf{N}_3 + \mathbf{N}_4 \quad (66)$$

where

$$\mathbf{N}_3 = \tfrac{1}{2}(\mathbf{N} - \mathbf{N}^\dagger) \quad (67)$$

and

$$\mathbf{N}_4 = \tfrac{1}{2}(\mathbf{N} + \mathbf{N}^\dagger) \quad (68)$$

and use the symmetric matrix $\mathbf{N}_4$ as an approximation for the matrix $\mathbf{G}^a$.

The above method for approximating the coupling matrices between adiabatic electronic states has the double advantage that the matrices used are independent of the method of orthogonalization and they also contain a contribution from the orthogonalization which generally has been ignored[47] in the literature.

We have of course still not obtained the total coupling between the electronic adiabatic states since we have not calculated the quantities $\vec{\mathbf{F}}^n$ and $\mathbf{G}^n$ and it is not clear what the relative importance of these matrices will be compared to the matrices $\mathbf{M}$ and $\mathbf{N}$. Tully has suggested[48] that "in low energy collision processes of interest to chemists, significant nonadiabatic behavior is invariably associated with a distinct and relatively sudden change of electronic configuration." Such behavior is described entirely by the second term of eq 60 and Tully and Preston have used this argument to justify neglecting the first term of eq 60 in applications.[48,49] It is possible in the case of a complete electronic basis set to define a diabatic basis such that the coupling matrices $\vec{\mathbf{F}}^d$ and $\mathbf{G}^d$ are identically zero so that all coupling between adiabatic states arises from derivatives of the unitary matrix which diagonalizes the electronic Hamiltonian $\mathbf{H}^d$ in that representation. However, such a representation[50] corresponds to electronic functions which are not allowed to vary as functions of the internuclear distance.[30,51,52] It is expected, therefore, that such a representation will give a very poor description of the molecule except in the limit of a very large basis set.

In the work presented here we have chosen a small basis set which is motivated by the physical properties of the molecules being considered and which we feel is large enough to include the properties of interest. Some indication of this is given in the discussion of adiabatic potential curves and bonding. Symmetric orthogonalization was then chosen to preserve this physical meaning in the orthogonal basis. This physical meaning will be important as a guide to making chemically motivated approximations[48,49] in treating the dynamics.

It is surely possible to use another method of orthogonalization such that the matrix $\vec{\mathbf{F}}^a$ may be written

$$\vec{\mathbf{F}}^a = \vec{\mathbf{F}}^d - i\mathbf{M}_2{}^d\hat{e}_R \quad (69)$$

where the matrix $\vec{\mathbf{F}}^d$ makes a smaller contribution to the coupling than does the matrix $\vec{\mathbf{F}}^s$ in the case of symmetric orthogonalization. The matrix $\mathbf{M}_2{}^d$ would then give a better description of the coupling than the matrix $\mathbf{M}_3$ defined in eq 64. However, until the matrix $\vec{\mathbf{F}}^n$ is calculated, it is not clear what method of orthogonalization yields the smallest matrix $\vec{\mathbf{F}}^d$ nor is it clear how much of the physical meaning is retained in the basis set for other methods of orthogonalization. The matrix $\vec{\mathbf{F}}^n$ can be calculated several ways.[53] One easy way is to make a numerical approximation to the derivative of eq 6. Then it reduces to a difference of overlap integrals. Thus if δ is small enough

$$\vec{\mathbf{F}}^n(R) \simeq -\frac{i}{2\mu\delta}[\langle\phi^n(R)|\phi^n(R+\delta)\rangle - \mathbf{S}]$$

Once the matrix $\vec{\mathbf{F}}^n$ has been calculated there is no need for approximation and just as in the treatment proposed here all methods of orthogonalization would be equivalent. We note, however, that the matrix $\vec{\mathbf{F}}^n$ does not generally become the matrix of null vectors in the large R limit[54] and new complications arise in the nuclear motion problem which do not arise using the present treatment. Previous workers have suggested some methods for overcoming these difficulties[53-55] and such methods must be considered if the effect of $\vec{\mathbf{F}}^n$ on the scattering is not negligible.

Added Note. The large positive corrections to the potential energy curves from the diagonal coupling terms near an avoided crossing (discussed above) are very interesting. A positive diagonal coupling term peaking at about 0.06 eV near an avoided crossing was observed previously for the E,F state of H_2.[56] Andresen and Nielsen observed very large positive coupling terms ("of the order of the potential depth" but with "an extremely narrow range") near an avoided crossing for some other excited states of H_2.[57]

VI. Summary

We have calculated potential energy curves and a major part of the coupling matrix elements in the adiabatic representation and more than one diabatic representation for several singlet and triplet states of NaH, KH, and MgH^+. We have discussed these results and compared them to each other and to previous work. For the latter comparison we emphasized the differences in wave functions used. The present calculations illustrate the functional forms of the coupling matrix elements as functions of internuclear distance more clearly than previous work.

Supplementary Material Available. Figures containing matrix elements $H_{ij}{}^s$, M_{ij}, and N_{ij} for the $^1\Sigma^+$ and $^3\Sigma^+$ states of MgH^+ as functions of internuclear distance will appear following these pages in the microfilm edition of this volume of the journal. Photocopies of the supplementary material from this paper only or microfiche (105 × 148 mm, 24× reduction, negatives) containing all of the supplementary material for this issue may be obtained from the Business Office, Books and Journal Division, American Chemical Society, 1155 16th St., N.W., Washington, D.C. 20036. Remit check or money order for $4.00 for photocopy or $2.50 for microfiche, referring to code number JPC-75-2745.

References and Notes

(1) (a) This article is based on the Ph.D. thesis of one of the authors (R.W.N.). This work was supported in part by the National Science Foundation. (b) Alfred P. Sloan Research Fellow.

(2) L. Landau, *Z. Phys. Sovjet.*, **2**, 46 (1932); C. Zener, *Proc. Roy. Soc. London, Ser. A*, **137**, 696 (1932); E. C. G. Stueckelberg, *Helv. Phys. Acta*, **5**, 369 (1932); W. R. Thorson, J. B. Delos, and S. A. Boorstein, *Phys. Rev. A*, **4**, 1052 (1971); J. B. Delos and W. R. Thorson, *Phys. Rev. A*, **6**, 728 (1972).
(3) D. R. Bates and T. J. M. Boyd, *Proc. Phys. Soc. London, Ser. A*, **69**, 910 (1956).
(4) R. Grice and D. R. Herschbach, *Mol. Phys.*, **27**, 159 (1974).
(5) Except where stated otherwise we use hartree atomic units where $m = e = \hbar = a_0 = 1$; the unit of energy is the hartree (1 hartree = 4.360×10^{-18} J = 27.21 eV) and the unit of length is the bohr (1 a_0 = 5.292×10^{-11} m). We also use the approximation $\mu_e \simeq m$.
(6) J. O. Hirschfelder and W. J. Meath, *Adv. Chem. Phys.*, **12**, 3 (1967).
(7) C. J. Ballhausen and A. E. Hansen, *Annu. Rev. Phys. Chem.*, **23**, 15 (1972).
(8) P. O. Löwdin, *Adv. Quantum Chem.*, **5**, 185 (1970).
(9) L. R. Kahn and W. A. Goddard, *J. Chem. Phys.*, **56**, 2685 (1972).
(10) H. Hellmann, *Acta Physicochim. URSS*, **1**, 913 (1935); H. Hellmann, *J. Chem. Phys.*, **3**, 61 (1935).
(11) P. Gombas, *Z. Phys.*, **94**, 473 (1935); **118**, 164 (1941).
(12) J. D. Weeks, A. Hazi, and S. A. Rice, *Adv. Chem. Phys.*, **16**, 283 (1969); J. N. Bardsley, *Case Stud. At. Phys.*, **4**, 299 (1974).
(13) D. G. Truhlar, *J. Comput. Phys.*, **10**, 123 (1972).
(14) L. Szasz and G. McGinn, *J. Chem. Phys.*, **42**, 2363 (1965).
(15) G. A. Hart and P. L. Goodfriend, *J. Chem. Phys.*, **53**, 448 (1970).
(16) W. H. E. Schwarz, *Theor. Chim. Acta*, **11**, 377 (1968).
(17) W. H. E. Schwarz, *Acta Phys. Acad. Sci. Hung.*, **27**, 391 (1969).
(18) W. H. E. Schwarz, *J. Chem. Phys.*, **54**, 1842 (1971).
(19) All experimental atomic energies, except for H^-, in this article are taken from the standard tables [C. E. Moore, *Natl. Bur. Stand. Circ.*, **No. 467** (1949)]. Since we are neglecting spin–orbit coupling, the P state energies are weighted averages of the observed $^2P_{1/2}$ and $^2P_{3/2}$ components. The H^- energy is taken from C. L. Pekeris, *Phys. Rev.*, **126**, 1470 (1962).
(20) J. C. Phillips and L. Kleinman, *Phys. Rev.*, **116**, 287 (1959).
(21) L. Szasz and G. McGinn, *J. Chem. Phys.*, **47**, 3495 (1967).
(22) J. Callaway and P. Laghos, *Phys. Rev.*, **187**, 192 (1969).
(23) H. F. Schaefer, III, "The Electronic Structure of Atoms and Molecules", Addison-Wesley, Reading, Mass., 1972, p 57.
(24) W. A. Goddard, *J. Chem. Phys.*, **48**, 1008 (1968).
(25) C. Froese, *Can. J. Phys.*, **41**, 1895 (1963).
(26) D. R. Bates and A. Damgaard, *Phil. Trans. R. Soc., Ser. A*, **242**, 101 (1949).
(27) H. F. Schaeffer, III, *J. Chem. Phys.*, **52**, 6241 (1970). The authors are grateful to Dr. K. C. Kulander for providing a copy of this program.
(28) A. Dalgarno, *Adv. Phys.*, **11**, 281 (1962).
(29) D. W. Marquardt, *J. Soc. Ind. Appl. Math.*, **11**, 431 (1963).
(30) R. W. Numrich, Ph.D. Thesis, University of Minnesota, Minneapolis, Minn., 1974.
(31) R. S. Mulliken, *Phys. Rev.*, **50**, 1028 (1936).
(32) A. G. Gaydon, "Dissociation Energies", 3rd ed, Chapman and Hall, London, 1968, p 102.
(33) M. E. Pillow, *Proc. Phys. Soc. London, Ser. A*, **62**, 237 (1949).
(34) Figures A1 through A6 will appear following this article in the microfilm edition of this volume of the journal. See paragraph at end of text regarding supplementary material.
(35) T. F. O'Malley, *Adv. At. Mol. Phys.*, **7**, 223 (1971).
(36) C. F. Melius, W. A. Goddard, and L. R. Kahn, *J. Chem. Phys.*, **56**, 3342 (1972); C. F. Melius and W. A. Goddard, *ibid.*, **56**, 3348 (1972).
(37) P. E. Cade and W. M. Huo, *J. Chem. Phys.*, **47**, 649 (1967).
(38) L. Szasz and G. McGinn, *J. Chem. Phys.*, **48**, 2997 (1968).
(39) T. G. Heil, S. V. O'Neil, and H. F. Schaeffer, III, *Chem. Phys. Lett.*, **5**, 253 (1970).
(40) F. E. Harris and H. H. Michels, *Int. J. Quantum Chem., Symp.*, **1**, 329 (1967).
(41) E. L. Lewis, L. F. McNamara, and H. H. Michels, *Phys. Rev. A*, **3**, 1939 (1971).
(42) R. E. Olson, F. T. Smith, and E. Bauer, *Appl. Opt.*, **10**, 1848 (1971).
(43) M. Oppenheimer, *J. Chem. Phys.*, **57**, 3899 (1972).
(44) F. London, *Z. Phys.*, **74**, 143 (1932); R. S. Berry, *J. Chem. Phys.*, **27**, 1288 (1957).
(45) L. Wolniewicz, *J. Chem. Phys.*, **45**, 515 (1966).
(46) S. A. Evans, J. S. Cohen, and N. F. Lane, *Phys. Rev. A*, **4**, 2235 (1971).
(47) M. J. Redmon and D. A. Micha, *Int. J. Quantum Chem., Symp.*, **8**, 253 (1974).
(48) J. C. Tully, *J. Chem. Phys.*, **59**, 5122 (1973).
(49) R. K. Preston and J. C. Tully, *J. Chem. Phys.*, **54**, 4297 (1971); J. C. Tully, *ibid.*, **60**, 3042 (1974).
(50) F. T. Smith, *Phys. Rev.*, **179**, 111 (1969).
(51) B. Andresen and S. E. Nielsen, *Mol. Phys.*, **21**, 523 (1971).
(52) H. Gabriel and K. Taulbjerg, *Phys. Rev. A*, **10**, 741 (1974).
(53) See, e.g., J. C. Browne, *Adv. At. Mol. Phys.*, **7**, 47 (1971), and references therein.
(54) See, e.g., D. W. Jepsen and J. O. Hirschfelder, *J. Chem. Phys.*, **32**, 1323 (1960); W. R. Thorson, *ibid.*, **42**, 3878 (1965); D. R. Bates and D. Sprevak, *J. Phys. B*, **4**, L47 (1971); J. C. Y. Chen, V. H. Ponce, and K. M. Watson, *ibid.*, **6**, 965 (1973); V. Sether Raman, W. R. Thorson, and C. F. Lebeda, *Phys. Rev. A*, **8**, 1316 (1973), and references therein.
(55) C. F. Melius and W. A. Goddard, III, *Chem. Phys. Lett.*, **15**, 524 (1972).
(56) S. Kolos and L. Wolniewicz, *J. Chem. Phys.*, **50**, 3228 (1969); W. Kolos, *Adv. Quantum Chem.*, **5**, 99 (1970).
(57) S. E. Nielsen, private communication. See also B. Andresen, Thesis, University of Copenhagen, Copenhagen, 1974, ref 51, and B. Andresen and S. E. Nielsen, *Mol. Phys.*, submitted for publication.

High-Resolution Electron Paramagnetic Resonance Study of Deuteration in Toluene Anion Radical

Suzanne Kowalski, Roger V. Lloyd,[1] and David E. Wood*

Department of Chemistry, University of Connecticut, Storrs, Connecticut 06268 *(Received June 13, 1975)*

Publication costs assisted by the Petroleum Research Fund

The individual ring proton hfs in ortho and meta monodeuterated toluene anion radical have been resolved by preparation with 2/1 THF/DME solvent and potassium at −90°C. The presence of deuterium does cause relatively large changes in the remaining proton hfs but the assignment of Bolton and Carrington (meta > ortho) is proven correct.

The EPR spectrum of the toluene anion radical was completely analyzed by Bolton and Carrington,[2] who assigned the 5.12-G hyperfine splittings (hfs) to the ortho protons, and the 5.45-G hfs to the meta protons, on the basis of the decrease in the total width of the spectrum upon deuteration at the ortho position. Since it has been found more recently that deuteration has a large perturbing effect upon the hfs of the benzene anion radical[3] because of vibronic interactions,[4] we decided to reinvestigate the spectra of toluene anions deuterated at both the ortho and the meta posi-